

EXPERIMENTAL RESULTS ON POTENTIAL MARKOV PARTITIONS FOR WANG SHIFTS

HARPER HULTS, HIKARU JITSUKAWA, CASEY MANN, AND JUSTIN ZHANG

ABSTRACT. In this article we discuss potential Markov partitions for three different Wang tile protosets. The first partition is for the order-24 aperiodic Wang tile protoset that was recently shown in the Ph.D. thesis of H. Jang to encode all tilings by the Penrose rhombs. The second is a partition for an order-16 aperiodic Wang protoset that encodes all tilings by the Ammann A2 aperiodic protoset. The third partition is for an order-11 Wang tile protoset identified by Jeandel and Rao as a candidate order-11 aperiodic Wang tile protoset. The emphasis is on some experimental methodology to generate potential Markov partitions that encode tilings. We also apply some of the theory developed by Labbé in analyzing such an experimentally discovered partition.

1. INTRODUCTION

1.1. Tilings and Aperiodic Protosets. A *tiling* of the Euclidean plane \mathbb{E}^2 is a collection $\{T_i\}$ of distinct sets called *tiles* (which are typically topological disks) such that $\cup T_i = \mathbb{E}^2$ and for all $i \neq j$, $\text{int}(T_i) \cap \text{int}(T_j) = \emptyset$. A *protoset* for a tiling \mathcal{T} is a collection of tiles \mathcal{T} such that each tile of \mathcal{T} is congruent to a tile in \mathcal{T} , in which case we say that \mathcal{T} *admits* the tiling \mathcal{T} . The *symmetry group* of a tiling \mathcal{T} is the set of rigid planar transformations $\mathcal{S}(\mathcal{T})$ such that $\sigma(\mathcal{T}) = \mathcal{T}$ for all $\sigma \in \mathcal{S}(\mathcal{T})$. If $\sigma(\mathcal{T})$ contains two nonparallel translations, we say that \mathcal{T} is *periodic*; otherwise, we say \mathcal{T} is *nonperiodic*. If \mathcal{T} admits at least one tiling of the plane and every such tiling is nonperiodic, we say that \mathcal{T} is an *aperiodic protoset*.

Aperiodic protosets are somewhat rare, and indeed, until the 1960s, no aperiodic protosets were known to exist. H. Wang famously conjectured that aperiodic protosets cannot exist [Wan61]; that is, Wang conjectured that any protoset that admits a tiling of the plane must admit at least one periodic tiling. Wang's conjecture was refuted in 1964 by his doctoral student, R. Berger, in his PhD thesis [Ber65; Ber66] where an aperiodic protoset consisting of over 20,000 edge-marked squares called Wang tiles was described. Wang tiles are a bit of a special case in the theory of tilings in that only translations are allowed in forming tilings from Wang tile protosets; if rotations and reflections are also allowed, then any single Wang tile admits periodic tilings of the plane, and so without this restriction the problem is trivial. Since Berger's original discovery, several lower-order aperiodic Wang tile protosets have been discovered, culminating in 2015 with the discovery by E. Jeandel and M. Rao [JR21] of an order-11 aperiodic Wang tile protoset. In this same work the authors proved that 11 is the minimum possible order for an aperiodic Wang tile protoset. The aperiodic Jeandel-Rao protoset is seen in Figures 1, and here we are using the same labeling for the Jeandel-Rao protoset as given by Labbé in [Lab21].

Aperiodic protosets of tiles other than Wang tiles are also known. In 1971, R. Robinson developed a way to encode the idea of Berger's original aperiodic protoset into an order-6 aperiodic protoset consisting of shapes with notched edges and modified corners (Figure 2a). In 1974, R. Penrose discovered an order-6 aperiodic protoset that he was later able to modify to produce an order-2 aperiodic protoset. There are a few varieties of the order-2 aperiodic Penrose protoset, one of which,

Date: July 2022.

2020 Mathematics Subject Classification. Primary 37B51; Secondary 37B10, 52C23.

Key words and phrases. Aperiodic tiling and Wang shift and SFT and Multidimensional SFT and Nonexpansive directions.

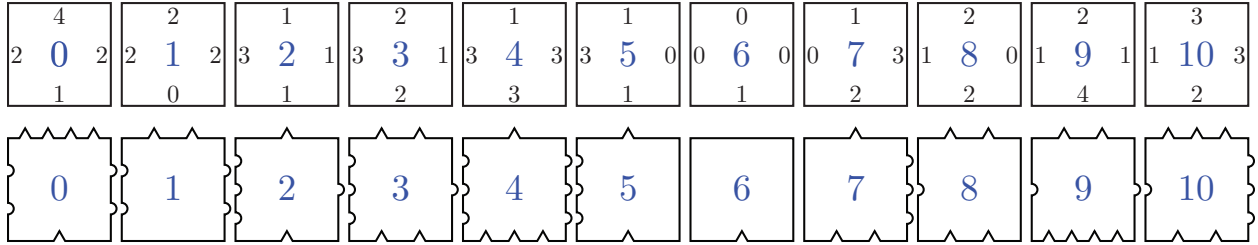


FIGURE 1. The Jeandel-Rao aperiodic Wang protoset \mathcal{T}_0 . The bottom row provides geometric matching rules for the prototiles in the top row.

called *P3* or the *Penrose rhombs*, is depicted in Figure 2b; this protoset will be discussed further in this article. More recently, in 2023 two singleton aperiodic protosets were discovered ([Smi+23b; Smi+23a]) - these “aperiodic monotiles” are called the *hat* (Figure 2c) and *spectre* (Figure 2d); we note that no edge-matching rules are needed to enforce nonperiodicity with the hat and spectre, unlike the Penrose rhombs, for example.

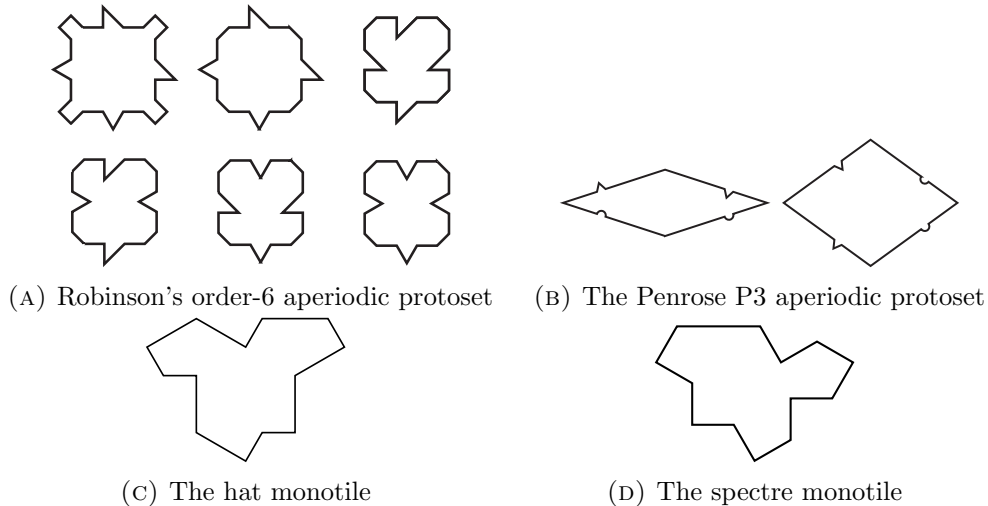


FIGURE 2. Some low-order aperiodic protosets

1.2. Labbé's Markov Partition for the Jeandel-Rao Protoset. Let $\mathcal{T}_0 = \{T_0, T_1, T_2, \dots, T_{10}\}$ be the aperiodic Jeandel-Rao Wang tile protoset (Figure 1). The set of all tilings admitted by \mathcal{T}_0 is called the *Jeandel-Rao Wang shift* and is denoted Ω_0 . In [Lab21], S. Labbé presented a special partition $\mathcal{P}_0 = \{P_0, P_1, \dots, P_{10}\}$ (Figure 3) of the two-dimensional torus \mathbf{T} , along with a \mathbb{Z}^2 action on \mathbf{T} , that together give rise to tilings in Ω_0 . Specifically, let $\varphi = (1 + \sqrt{5})/2$ be the golden mean and let Γ_0 be the lattice in \mathbb{R}^2 generated by $(\varphi, 0)$ and $(1, \varphi + 3)$. Then the partitioned torus is $\mathbf{T} = \mathbb{R}^2/\Gamma_0$ and the \mathbb{Z}^2 action R_0 on \mathbf{T} is defined by $R_0^n(\mathbf{x}) = \mathbf{x} + \mathbf{n} \pmod{\Gamma_0}$.

Here we describe how the partition \mathcal{P}_0 of \mathbf{T} and the action R_0 encode tilings by \mathcal{T}_0 . Let $p \in \mathbf{T}$ and consider the orbit $\mathcal{O}_{R_0}(p) = \{R_0^n(p) : \mathbf{n} \in \mathbb{Z}^2\}$. Then $\mathcal{O}_{R_0}(p)$ corresponds to a tiling in Ω_0 in the following way:

$$T_i \in \mathcal{T}_0 \text{ is located at position } \mathbf{n} \text{ iff } R_0^n(p) \in P_i.$$

This idea is depicted in Figure 3. There are several technical details that Labbé proved so that the correspondence between orbits of points in the partitioned torus corresponds to tilings in an unambiguous way, but this is the gist of it. It is interesting - even somewhat amazing - that most tilings admitted by \mathcal{T}_0 are encoded by \mathcal{P}_0 and R_0 !

In this article, we present some partitions, discovered experimentally, that are analogous to the Markov partition \mathcal{P}_0 for the Jeandel-Rao protoset, but for other Wang tile protosets. Further, we discuss how to identify other potential Markov partitions for Wang shifts in which tilings exhibit “golden rotational” behavior similar to R_0 with \mathcal{P}_0 . We will also discuss theoretical framework described by Labbé in [Lab21] and apply it to one of these new partitions in an effort to describe the full space of tilings arising from the partition.

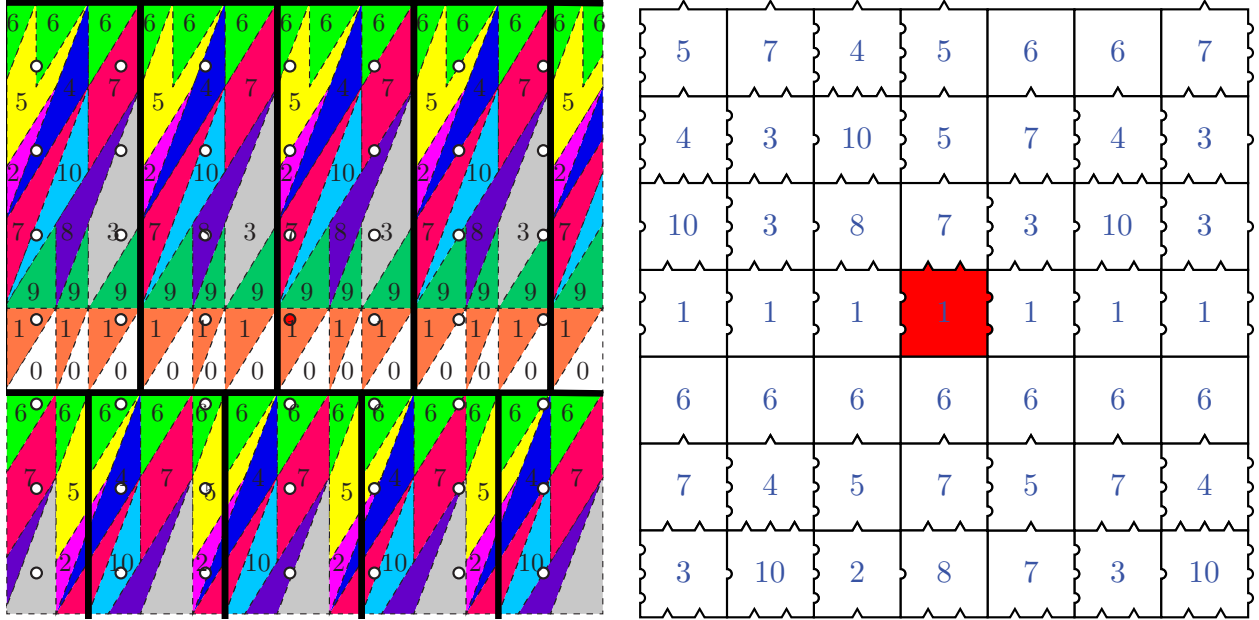


FIGURE 3. Labbé’s partition \mathcal{P}_0 of the torus \mathbf{T} is outlined by the heavy black line. The orbit of the red point \mathbf{p} under the \mathbb{Z}^2 -action R_0 defined by $R_0^n(\mathbf{p}) = \mathbf{p} + \mathbf{n}$ (the set of white points) corresponds to a Wang tiling in Ω_0 , depicted at right.

2. LABBÉ’S CONSTRUCTION

While we are focussed on an experimental approach in this article, it will be necessary to describe some of the technical details of Labbé’s construction, which are described in the language of dynamical systems. For now, we want to keep this discussion as non-technical as possible to focus on the big picture ideas, and we will provide more technical aspects in Appendix A. In that spirit, let us start by describing Wang tilings in the language of dynamical systems. This begins by defining Wang tilings in a very symbolic way.

2.1. Spaces of Wang Tilings as Dynamical Systems. Geometrically, a *Wang tile* is a square with labeled (or colored) sides that serve as edge matching rules; two Wang tiles may meet along an edge if corresponding labels match. In forming a *Wang tiling* from copies of tiles in a protoset of Wang tiles, we allow only translates of the prototiles to be used, and we require that the tiles to meet edge-to-edge, respecting the matching rules. The edge-to-edge matching rules and restriction to translations can always be enforced geometrically, as in Figure 1. Wang tilings can be aligned with the integer lattice \mathbb{Z}^2 so that each tile has its lower left-hand corner in \mathbb{Z}^2 , and thus we may view a Wang tiling as a decoration of \mathbb{Z}^2 such that each point of \mathbb{Z}^2 is “colored” with a single tile.

More formally, a Wang tile can be represented as a tuple of four colors $(r, t, \ell, b) \in V \times H \times V \times H$ where V and H are finite sets (the vertical and horizontal colors, respectively). For any Wang tile $T = (r, t, \ell, b)$, let $\text{Right}(T) = r$, $\text{Top}(T) = t$, $\text{Left}(T) = \ell$, and $\text{Bottom}(T) = b$ be the colors of the right, top, left, and bottom sides of τ , respectively. Let $\mathcal{T} = \{T_0, T_1, \dots, T_{n-1}\}$ be a protoset of Wang

tiles. In forming a tiling with the protoset \mathcal{T} , we will think of the prototiles of \mathcal{T} as symbols used to label the integer lattice \mathbb{Z}^2 . This motivates us to define

$$\mathcal{T}^{\mathbb{Z}^2} = \{x: \mathbb{Z}^2 \rightarrow \mathcal{T}\}$$

to be the **configuration space** of \mathcal{T} , and each element $x \in \mathcal{T}^{\mathbb{Z}^2}$ is called a **configuration**. We will use the notation $x_{\mathbf{n}} = x(\mathbf{n})$ to indicate the value of x at $\mathbf{n} \in \mathbb{Z}^2$ so that if $x_{\mathbf{n}} = T_i$ we understand that tile T_i is located at position \mathbf{n} (i.e., oriented so that its corners lie in \mathbb{Z}^2 and the lower left-hand corner is at \mathbf{n}). It is possible that a configuration in $\mathcal{T}^{\mathbb{Z}^2}$ does not represent a valid tiling; so far, this construction does not account for the matching rules of the tiles. To account for the matching rules, we define a configuration x to be **valid** if for every $\mathbf{n} \in \mathbb{Z}^2$, we have $\text{Right}(x_{\mathbf{n}}) = \text{Left}(x_{\mathbf{n}+(1,0)})$ and $\text{Top}(x_{\mathbf{n}}) = \text{Bottom}(x_{\mathbf{n}+(0,1)})$. The **Wang shift** of \mathcal{T} is the set $\Omega_{\mathcal{T}}$ of all valid configurations in $\mathcal{T}^{\mathbb{Z}^2}$. Thus, $\Omega_{\mathcal{T}}$ captures in a symbolic way the set of all valid Wang tilings admitted by the Wang tile protoset \mathcal{T} .

A **topological dynamical system** consists of a topological space X and a group G that acts on X via a continuous function $S: G \times X \rightarrow X$, and is denoted by a triple (X, G, S) . For fixed $g \in G$, let $S^g: X \rightarrow X$ be defined by $S^g(x) = S(g, x)$. The **orbit** of a point $x \in X$ under the action of S on G is the set $\mathcal{O}_S(x, G) = \{S^g(x) : g \in G\}$, and when the group G is understood by context, we will shorten this notation to just $\mathcal{O}_S(x)$. We say S **acts freely** on X if for all $x \in X$, $S^g(x) = x$ if and only if $g = e$ where $e \in G$ is the group identity element.

Let $\sigma: \mathbb{Z}^2 \times \mathcal{T}^{\mathbb{Z}^2} \rightarrow \mathcal{T}^{\mathbb{Z}^2}$ be defined by $\sigma^{\mathbf{n}}(x_{\mathbf{m}}) = x_{\mathbf{m}+\mathbf{n}}$. We call σ the \mathbb{Z}^2 **shift action** on $\mathcal{T}^{\mathbb{Z}^2}$; the terminology ‘‘shift action’’ is accurately descriptive here since, for each $\mathbf{n} \in \mathbb{Z}^2$ and $x \in \mathcal{T}^{\mathbb{Z}^2}$, $\sigma^{\mathbf{n}}(x)$ is a translation of x by \mathbf{n} . By placing the appropriate metric on $\mathcal{T}^{\mathbb{Z}^2}$, it is not too hard to see that $\Omega_{\mathcal{T}} \subseteq \mathcal{T}^{\mathbb{Z}^2}$ is a topological space so that $(\Omega_{\mathcal{T}}, \mathbb{Z}^2, \sigma)$ satisfies the definition of being a topological dynamical system. Moreover, $(\Omega_{\mathcal{T}}, \mathbb{Z}^2, \sigma)$ is a special kind of topological dynamical system called a **shift of finite type** (see Appendix A).

If σ acts freely on $\Omega_{\mathcal{T}}$, we say that $\Omega_{\mathcal{T}}$ is an **aperiodic shift**, and we say that a Wang protoset \mathcal{T} is an **aperiodic protoset** if the corresponding Wang shift $\Omega_{\mathcal{T}}$ is nonempty and aperiodic. Notice that this definition for aperiodic protoset agrees with with more general definition given in Section 1.1 if we restrict the allowable symmetries to translations only.

2.2. Labbé’s Partition-Based Dynamical System of Tilings. Here we will provide the broad strokes of Labbé’s [Lab21] general approach and construction of the dynamical system $(\mathcal{X}_{\mathcal{P},R}, \mathbb{Z}^2, \sigma)$ that is based on a partition \mathcal{P} of a compact topological space \mathbf{T} and a \mathbb{Z}^2 action R on \mathbf{T} . The space $\mathcal{X}_{\mathcal{P},R}$ is the set of tilings encoded by the partition \mathcal{P} and the action R , as exemplified by Figure 3. We will relegate much of the more technical details to Appendix A. The main point is that methodologies are described in [Lab21] that can be used to prove when \mathcal{P} and R produce a space $\mathcal{X}_{\mathcal{P},R}$ that is reasonable subspace (or subshift) of the space of all valid tilings $\Omega_{\mathcal{T}}$ admitted by \mathcal{T} .

First, let \mathbf{T} be a compact metric space and let $I_n = \{0, 1, \dots, n-1\}$. A collection $\mathcal{P} = \{P_i\}_{i \in I_n}$ of disjoint open sets with $\mathbf{T} = \cup_{i \in I_n} \overline{P_i}$ is called a **topological partition** of \mathbf{T} , and the sets $P_i \in \mathcal{P}$ are called the **atoms** of the partition. Let $\mathcal{P} = \{P_i\}_{i \in I_n}$ is a topological partition of \mathbf{T} , and let $\mathcal{T} = \{T_i\}_{i \in I_n}$ be a protoset of Wang tiles having the same indexing set I_n as \mathcal{P} . Let R be a \mathbb{Z}^2 action on \mathbf{T} . Then $(\mathbf{T}, \mathbb{Z}^2, \mathbb{R})$ is a topological dynamical system, and with \mathbf{T} so partitioned by \mathcal{P} , the hope is that the orbit of a point $p \in \mathbf{T}$ will ‘‘spell out’’ a tiling in $\Omega_{\mathcal{T}}$. More precisely, for each $p \in \mathbf{T}$, we can consider the orbit $\mathcal{O}_R(p) = \{R^{\mathbf{n}}(p) : \mathbf{n} \in \mathbb{Z}^2\}$, and for each $\mathbf{n} \in \mathbb{Z}^2$, define the configuration $x: \mathbb{Z}^2 \rightarrow \mathcal{T}$ in $\mathcal{T}^{\mathbb{Z}^2}$ by

$$x_{\mathbf{n}} = T_i \text{ if and only if } R^{\mathbf{n}}(p) \in P_i.$$

The configuration x may not be not well defined because for some $\mathbf{n} \in \mathbb{Z}^2$, the point $R^{\mathbf{n}}(p)$ may lie on the boundary of more than one atom of P_i . However, Labbé [Lab21] was able prove that this ambiguity can be removed in the following way: By specifying a direction \mathbf{v} that is not parallel to

any of the sides of the atoms of the partition, then if a point $a \in \mathcal{O}_R(p)$ falls on the boundary of an atom, the choice of tile associated with that point is the one in the direction of \mathbf{v} from a . In this way, each point $p \in \mathbf{T}$ can be associated uniquely with a configuration $x \in \mathcal{T}^{\mathbb{Z}^2}$, thereby defining a mapping $\text{SR}^{\mathbf{v}} : \mathbf{T} \rightarrow \mathcal{T}^{\mathbb{Z}^2}$ (“ SR ” for “symbolic representation”). With this map properly defined, we obtain the space of interest, $\mathcal{X}_{\mathcal{P},R}$, as the topological closure of the image of $\text{SR}^{\mathbf{v}}$:

$$\mathcal{X}_{\mathcal{P},R} = \overline{\text{SR}^{\mathbf{v}}(\mathbf{T})}.$$

Labbé [Lab21] shows that the choice of \mathbf{v} doesn’t actually matter after taking the topological closure, so the space $\mathcal{X}_{\mathcal{P},R}$ is not dependent on \mathbf{v} . Figure 3 is worth a thousand words in understanding the essential function of SR . In that figure, we see how the points of the orbit of a point p in the torus forms a *configuration* of Wang tiles.

We pause here to point out that the space $\mathcal{X}_{\mathcal{P},R}$ is fully defined in more technical terms in [Lab21] that facilitate the use of the tools of dynamical systems to prove that if the partition \mathcal{P} and the action R satisfy reasonable technical properties, the partitioned system $(\mathbf{T}, \mathbb{Z}^2, R)$ gives rise to $(\mathcal{X}_{\mathcal{P},R}, \mathbb{Z}^2, \sigma)$ along with morphisms going both directions. With such formalisms in place, important properties of the space $(\mathcal{X}_{\mathcal{P},R}, \mathbb{Z}^2, \sigma)$ can be determined. For example, we are interested in knowing when $(\mathcal{X}_{\mathcal{P},R}, \mathbb{Z}^2, \sigma)$ is shift of finite type, which is an important property that a Wang shift has. Another important property is minimality of the subshift, which can be deduced from properties of the partition and action.

At this point, it may be believable that $\mathcal{X}_{\mathcal{P},R}$ is a reasonable subset of $\mathcal{T}^{\mathbb{Z}^2}$, so configurations of $\mathcal{X}_{\mathcal{P},R}$ can be seen as potential valid configurations (i.e. tilings), but it should not be clear at all how the partition “knows” what the edge matching rules are and how orbits of points correspond to *valid tilings* that respect the matching rules of the prototiles of \mathcal{T} . This is where some magic occurs in the Labbé construction. The magic is that the partition \mathcal{P} needs to be a refinement of four other partitions $\mathcal{P}_r, \mathcal{P}_t, \mathcal{P}_\ell,$ and \mathcal{P}_b called *side partitions* that encode the matching rules of prototiles in \mathcal{T} . With these side partitions suitably defined, the main partition \mathcal{P} is defined as $\mathcal{P} = \mathcal{P}_r \cap \mathcal{P}_t \cap \mathcal{P}_\ell \cap \mathcal{P}_b$. With \mathcal{P} so defined, and checking that \mathcal{P} has certain necessary dynamical properties, it is argued in [Lab21] that $\mathcal{X}_{\mathcal{P},R} \subseteq \Omega_{\mathcal{T}}$. That is, the configurations generated from orbits of points in the partitioned set \mathbf{T} are valid tilings! We use the word “magic” here to describe the process of finding \mathcal{P} because there is no simple formula for finding such a partition. For a given Wang protoset \mathcal{T} , the partition may be found through some educated guesswork and the help of computers. In the next section, we will describe an experimental approach to finding partitions.

3. FINDING PARTITIONS EXPERIMENTALLY

Let us return to the Jeandel-Rao aperiodic protoset and Labbé’s corresponding Markov partition from Figure 3. Recall that in this construction we have $\mathbf{T} = \mathbb{R}^2/\Gamma_0$ where Γ_0 is generated by $(\varphi, 0)$ and $(1, \varphi + 3)$. Given a tiling $x \in \Omega_{\mathcal{T}_0}$, we will attempt to recover the partition \mathcal{P}_0 . Suppose that $x \in \Omega_0$ is “generated” from the orbit of a point $p \in \mathbf{T}$, using the partition \mathcal{P}_0 and the action R_0 . Without loss of generality, we may (by shifting the orientation of the partition \mathcal{P}_0) suppose that $p = \mathbf{0} = (0, 0)$. For each $\mathbf{n} \in \mathbb{Z}^2$, let $t_{\mathbf{n}} = R_0^{\mathbf{n}}(\mathbf{0})$. By definition of R_0 , we have

$$(1) \quad t_{\mathbf{n}} = \mathbf{n} \pmod{\Gamma_0}.$$

Recall the manner in which the partition \mathcal{P}_0 encodes the tiling: If $t_{\mathbf{n}} \in P_i \in \mathcal{P}_0$, then a copy of prototile $T_i \in \mathcal{T}_0$ is located at position \mathbf{n} .

Now, working backward, suppose we have a tiling x generated by the orbit $\mathcal{O}_{R_0}(\mathbf{0})$, but after generating x , let us pretend that we have lost all knowledge of the partition. If we colored the points $t_{\mathbf{n}}$ according to the label of the tile located at position \mathbf{n} , then the colored set of points

$$(2) \quad \mathcal{P}_{\text{dots}} = \{t_{\mathbf{n}} \in \mathbf{T} : n \in \mathbb{Z}^2, t_{\mathbf{n}} \text{ has color } i \text{ if } T_i \text{ is located at position } \mathbf{n}\}$$

would appear as a dense set of points in the rectangle $[\varphi, 0] \times [1, \varphi + 3]$, and the coloring of the points $t_{\mathbf{n}}$ would reveal the partition \mathcal{P}_0 .

Our goal here is to demonstrate that a partition associated with a Wang shift can be revealed by looking at specific tilings in the Wang shift without prior knowledge of the partition. By Equation 1, for each $\mathbf{n} \in \mathbb{Z}^2$, there exists some $\mathbf{a}_{\mathbf{n}} \in \mathbb{Z}^2$ such that

$$(3) \quad t_{\mathbf{n}} = \mathbf{n} + A\mathbf{a}_{\mathbf{n}}$$

where

$$A = \begin{pmatrix} \varphi & 1 \\ 0 & \varphi + 3 \end{pmatrix}$$

is the matrix whose columns are the generating vectors of Γ_0 . From Equation 3, we obtain $A^{-1}\mathbf{n} = A^{-1}t_{\mathbf{n}} - \mathbf{a}_{\mathbf{n}}$. Because $\mathbf{a}_{\mathbf{n}} \in \mathbb{Z}^2$, it follows that

$$(4) \quad A^{-1}\mathbf{n} \pmod{\mathbb{Z}^2} = A^{-1}t_{\mathbf{n}} \pmod{\mathbb{Z}^2}.$$

Let

$$\mathcal{P}'_{\text{dots}} = \{A^{-1}\mathbf{n} \pmod{\mathbb{Z}^2} : \mathbf{n} \in \mathbb{Z}^2\},$$

and assign to each $p_{\mathbf{n}} = A^{-1}\mathbf{n} \in \mathcal{P}'_{\text{dots}}$ the color i if a copy of prototile T_i is located at position \mathbf{n} . From Equation 4, we see that the set $\mathcal{P}'_{\text{dots}}$ is just a linearly transformed copy of the original dense set of colored points $\mathcal{P}_{\text{dots}}$, and recall that $\mathcal{P}_{\text{dots}}$ reveals the partition \mathcal{P}_0 . *Therefore, we see that $\mathcal{P}'_{\text{dots}}$, being a linear transformation of $\mathcal{P}_{\text{dots}}$, reveals a partition \mathcal{P}' that is essentially equivalent to the original \mathcal{P}_0 .*

If the only knowledge we have at the beginning of this process is that of a tiling or a large finite portion of a tiling (perhaps generated by a computer algorithm), then we may not be immediately privy to the matrix A (i.e., the generating vectors of the lattice that forms the torus) whose inverse we would use to pull back the tiling to obtain a partition, but the tiling itself may give clues about this matrix. In fact, Labbé discovered the partition in exactly this way - by noticing some Sturmian-like patterns in the rows of a large patch of a Jeandel-Rao tiling that suggested the correct vectors by which to “mod-out.” *Finding the matrix A is the key to this strategy.*

To see how this experimental approach reveals the partition (once you have guessed the correct generating vectors for the lattice), let us first use Labbé’s Sagemath package ([Lab23]) to produce a tiling of a given size. Here we produce a 100x100 patch of a Jeandel-Rao Wang tiling:

```

1  from slabbe import WangTileSet
2
3  tiles = [(2,4,2,1), (2,2,2,0), (1,1,3,1), (1,2,3,2), (3,1,3,3),
4  ...: (0,1,3,1), (0,0,0,1), (3,1,0,2), (0,2,1,2), (1,2,1,4), (3,3,1,2)]
5
6  T0 = WangTileSet(tiles)
7
8  # This produces a 100x100 tiling from the Jeandel-Rao protoset in which the
9  bottom row consists only of copies of prototile 4
10 x = 100
11 y = 100
12 preassigned_tiles = {(a,0):4 for a in range(x)};
13 S = T0.solver(x,y,preassigned_tiles=preassigned_tiles)
14 %time tiling = S.solve(solver='glucose')
```

Next, from the tiling so produced, we can pull back the points of the tiling to the unit square and color each using the label of the tile from which it came.

```

1  # This produces the pull back of the tiling into torus (quotient of the unit
2  square) in which the color of the pulled-back point is the label of the tile
3  from which it came.
4  p = (1+sqrt(5))/2;
5  M = matrix.column([[p,0],[1,p+3]]);
6  P = tiling.plot_points_on_torus(M.inverse(),pointsize=5)
7  show(P,aspect_ratio = 1)
```

Here is the picture so produced:

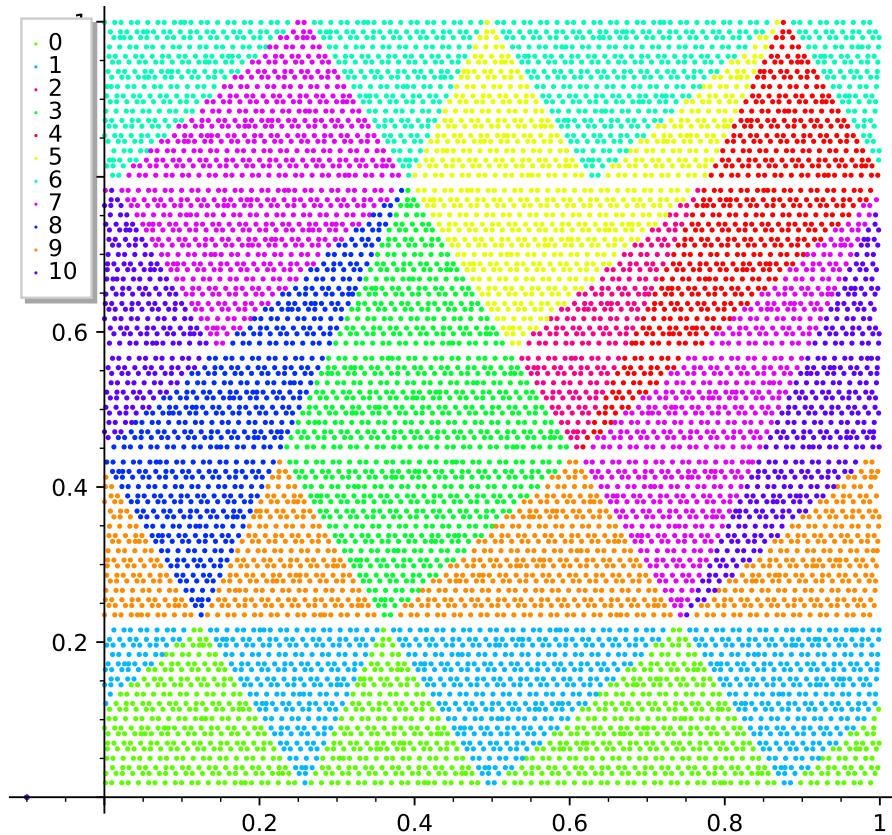


FIGURE 4. The result of applying A^{-1} to each tile location in a 100x100 sized patch of a Jeandel-Rao Wang tiling and coloring each point according to the label of the corresponding tile.

Comparing Figures 3 and 4, we see that the dot pattern does indeed capture the atoms of the original partition. It should be noted here that the tiling used to generate the colored dot pattern was not produced using the partition \mathcal{P}_0 ; instead, it was produced using the Glucose solver, which implements a brute force method to finding a tiling. This suggests that the partition is fundamental to the space Ω_0 , which is the main thrust of what Labbé proved in [Lab21].

4. THE PENROSE AND AMMANN WANG SHIFTS

In [GS87, Section 11.1], the authors discuss methods for converting low-order aperiodic protosets into low-order aperiodic Wang tile protosets, including the order-2 Penrose aperiodic protosets P2 and P3 and the order-2 Ammann aperiodic protoset A2. In particular, there we find an outline of how to convert Penrose tile protosets to two different aperiodic Wang tile protosets - one of order 24 (from P3) and one of order 16 (from P2). We also find that the Ammann A2 protosets can be converted to an order 16 Wang tile protoset, which, interestingly, is the exact same order-16 Wang tile protoset obtained from the Penrose P3 protoset, suggesting that P2 and A2 are really the same on some fundamental level. More recently, in H. Jang's recent Ph.D. thesis [Jan21, Lemma 6.2.2, p. 75], it was shown that any tiling by Penrose rhombs P3 is equivalent to a Wang tiling from the set of 24 Wang tiles mentioned above.

4.1. The Order-24 Penrose Wang Tile Protoset. Following the method suggested in [GS87, Section 11.1], a tiling by the Penrose rhombs (P3) can be converted to a tiling by Wang tiles using the patches of tiles shown in Figure 5. This protoset of 24 Wang tiles, as was proven in [Jan21], produces tilings in exact correspondence with the tilings produced by the P3 protoset.

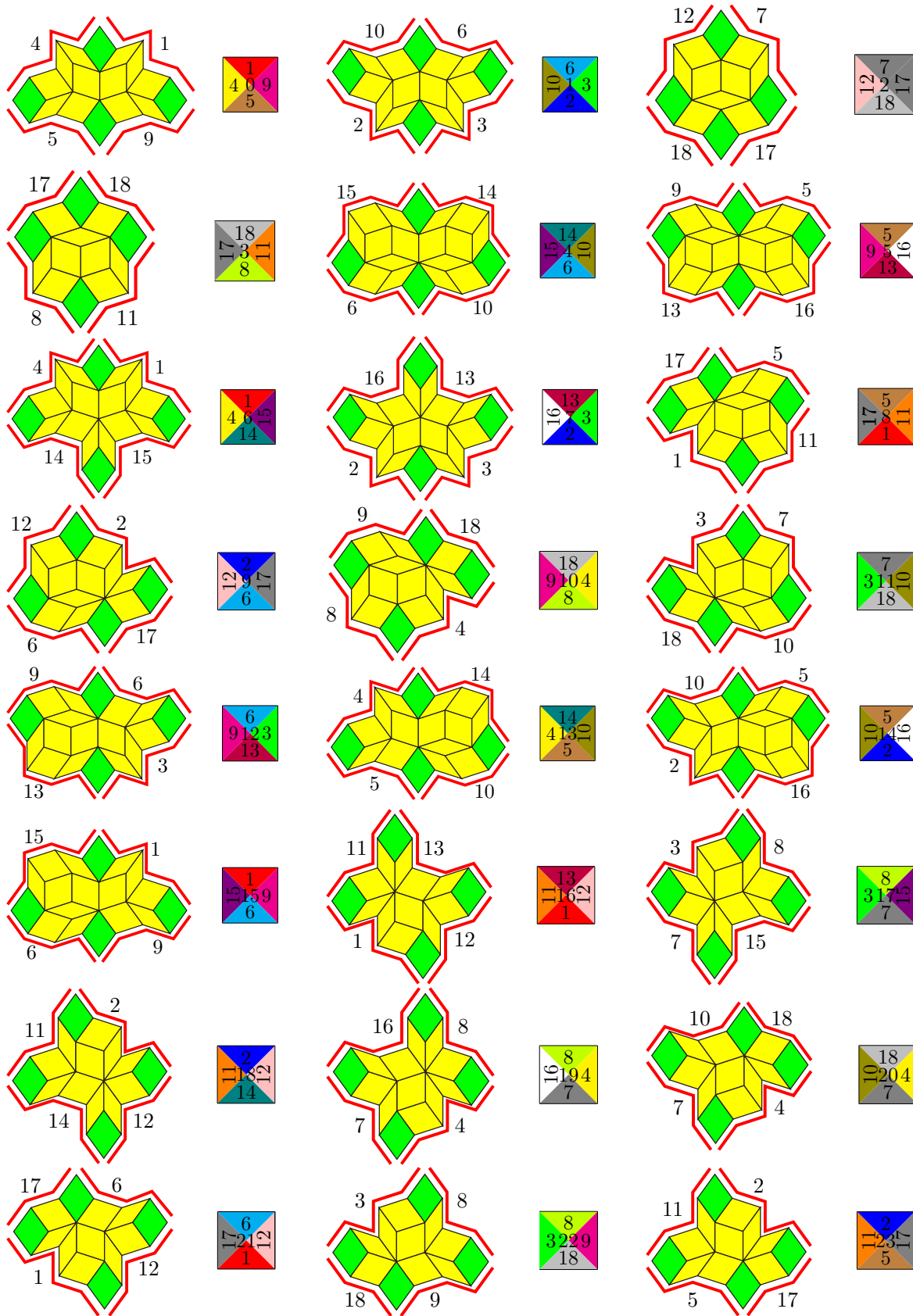
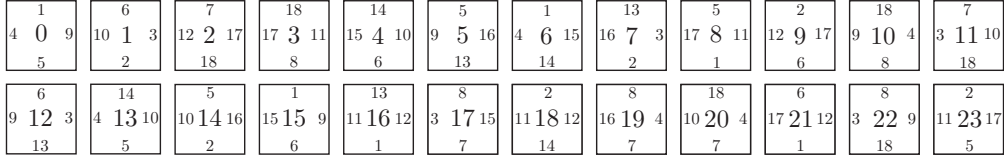


FIGURE 5. Patches of Penrose rhomb tilings and their corresponding Wang tiles. Red arcs with the same label are translates of one another, and so these labels correspond to colors the sides of the Wang tiles.

FIGURE 6. The order-24 aperiodic Wang protoset, \mathcal{T}_{24} corresponding to P3.

Let the protoset of Figure 6 be denoted by \mathcal{T}_{24} . We may use the computer to produce a large patch of tiling, and then using a matrix

$$A_{24} = \begin{pmatrix} \varphi & 0 \\ 0 & \varphi \end{pmatrix},$$

we can produce a dot pattern that reveals a partition for $\Omega_{\mathcal{T}_{24}}$.

```

1 Penrose24 = [(9,1,4,5), (3,6,10,2), (17,7,12,18), (11,18,17,8),
2             (10,14,15,6), (16,5,9,13), (15,1,4,14), (3,13,16,2),
3             (11,5,17,1), (17,2,12,6), (4,18,9,8), (10,7,3,18),
4             (3,6,9,13), (10,14,4,5), (16,5,10,2), (9,1,15,6),
5             (12,13,11,1), (15,8,3,7), (12,2,11,14), (4,8,16,7),
6             (4,18,10,7), (12,6,17,1), (9,8,3,18), (17,2,11,5)]
7 Pen24 = WangTileSet(Penrose24)
8 PenSol24 = Pen24.solver(130,130)
9 Pen24_tiling = PenSol24.solve(solver='glucose')
10
11 A = matrix.column([[p,0],[0,p]])
12 G = Pen24_tiling.plot_points_on_torus(A.inverse())
13 show(G,aspect_ratio=1,figsize=8)

```

From this dot pattern, we can guess at the exact slopes of the lines and produce an exact partition of the torus $\mathbf{T} = \mathbb{R}^2 \pmod{\mathbb{Z}^2}$, viewed as a quotient of the unit square. We have created such a partition in Figure 8. To simplify things, at right Figure 8 we have scaled the partition by a factor of φ to obtain a partition \mathcal{P}_{24} , and we may consider the torus $\mathbf{T} = \mathbb{R}^2 \pmod{\Gamma_{24}}$ where $\Gamma_{24} = \langle (\varphi, 0), (0, \varphi) \rangle$ with \mathbb{Z}^2 action R_{24} defined on \mathbf{T} by $R_{24}^{\mathbf{n}}(p) = p + \mathbf{n} \pmod{\mathbf{T}}$. From these ingredients, we can now consider the space $\mathcal{X}_{\mathcal{P}_{24}, R_{24}}$ and testable hypotheses concerning that space that lends itself to the techniques developed by Labbé in [Lab21], such as:

- Are configurations in $\mathcal{X}_{\mathcal{P}_{24}, R_{24}}$ always valid tilings in $\Omega_{\mathcal{T}_{24}}$? I.e., Is $\mathcal{X}_{\mathcal{P}_{24}, R_{24}} \subseteq \Omega_{\mathcal{T}_{24}}$?
- Is $\mathcal{X}_{\mathcal{P}_{24}, R_{24}}$ a shift of finite type?
- Is $\mathcal{X}_{\mathcal{P}_{24}, R_{24}}$ minimal in $\Omega_{\mathcal{T}_{24}}$?
- Is it true that $\mathcal{X}_{\mathcal{P}_{24}, R_{24}} = \Omega_{\mathcal{T}_{24}}$, so that the partition \mathcal{P}_{24} produces all possible Penrose tilings?
- Will $\mathcal{X}_{\mathcal{P}_{24}, R_{24}}$ exhibit nonexpansive directions, as corresponding space $\mathcal{X}_{\mathcal{P}_0, R_0}$ did for the Jeandel-Rao shift?

We will pursue questions such as these in Appendix B, but for now, we will continue with this experimental approach to finding a few other potential interesting partitions for Wang tile protosets.

4.2. The Order-16 Ammann A2 Wang Tile Protoset. The Ammann A2 order-2 aperiodic protoset is shown in Figure 9. Notice at bottom in Figure 9 that the tiles are adorned with red and blue lines called *Ammann bars*. The matching rule is that when two copies of tiles from A2 meet, Ammann bars of the same color must continue in a straight line. In Figure 10, we see how the matching rules are enforced in a small patch of tiling for the A2 protoset.

The key to converting the A2 protoset to a Wang tile protoset of order 16 is to consider all of the possible rhombi formed from the red lines, with the blue lines serving as the matching rules for

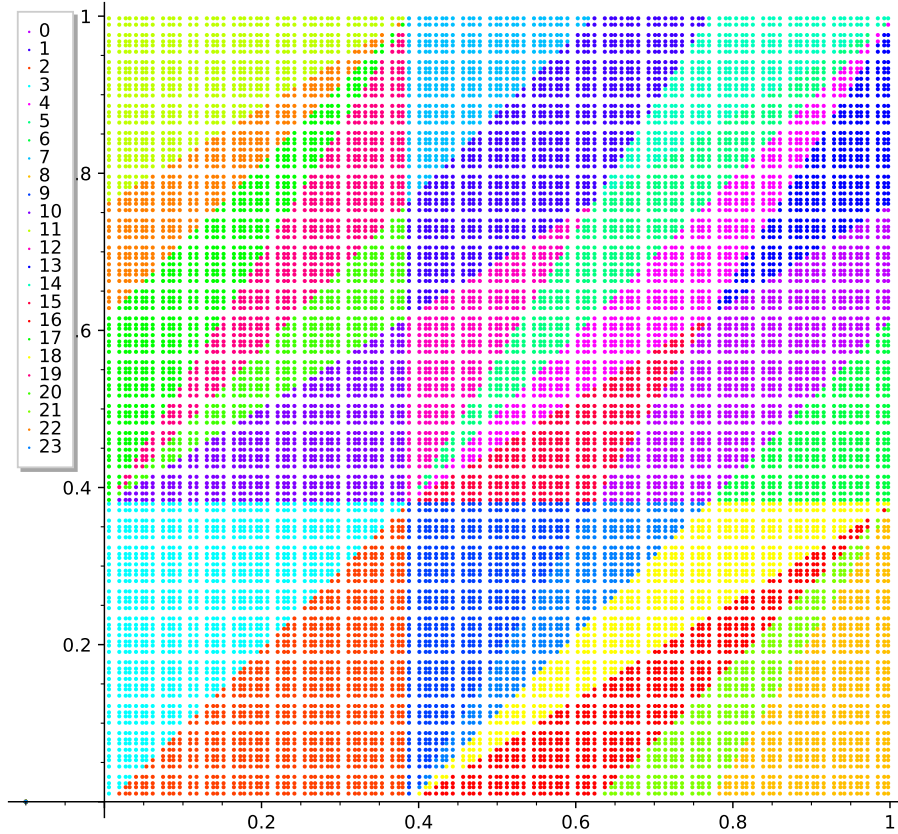


FIGURE 7. The result of applying A^{-1} to each tile location in a 130×130 sized patch of a \mathcal{T}_{24} tiling and coloring each point according to the label of the corresponding tile.

the red rhombi, as explained in In [GS87, Section 11.1]. The protoset so produced, \mathcal{T}_{16} , is shown in Figure 11.

Again, as we did with the \mathcal{T}_{24} , we can use the computer to produce a large patch of tiling, and with the appropriate choice of matrix, we can pull the tiling back onto a torus and see a dot pattern that indicates that a partition underlies the protoset. Indeed, using

$$A_{16} = \begin{pmatrix} \varphi & 0 \\ 0 & \varphi \end{pmatrix},$$

we obtain the nice dot pattern shown in Figure 12. Interestingly, we see not only that $A_{24} = A_{16}$, but also that the dot patterns for \mathcal{T}_{24} and \mathcal{T}_{16} align - the pattern for P3 seems to be a refinement of the one for A2 (Figure 13). This is not coincidental. In [GS87, Section 11.1] it is pointed out that \mathcal{T}_{16} can be derived from the Penrose darts and kites (P2) protoset using the idea of Ammann bars.

From the dot pattern obtained for \mathcal{T}_{16} , we can determine the exact equations of the lines to get a partition \mathcal{P}_{16} , as shown in Figure 14. We have scaled the partitioned torus for \mathcal{T}_{16} by a factor of φ (as we did for \mathcal{T}_{24}). Define the torus \mathbf{T} identifying opposites sides of this square $[0, \varphi] \times [0, \varphi]$ and define the \mathbb{Z}^2 action R_{16} on \mathbf{T} by $R_{16}^n(p) = p + \mathbf{n} \pmod{\mathbf{T}}$. We may now consider the space $\mathcal{X}_{\mathcal{P}_{16}, R_{16}}$ and consider questions like those outlined in Subsection 4.1.

4.3. Testing $\mathcal{X}_{\mathcal{P}_{24}, R_{24}}$ and $\mathcal{X}_{\mathcal{P}_{16}, R_{16}}$. Before considering more technical theoretical questions about $\mathcal{X}_{\mathcal{P}_{24}, R_{24}}$ and $\mathcal{X}_{\mathcal{P}_{16}, R_{16}}$, we will test, experimentally, if the configurations in these spaces seem to be

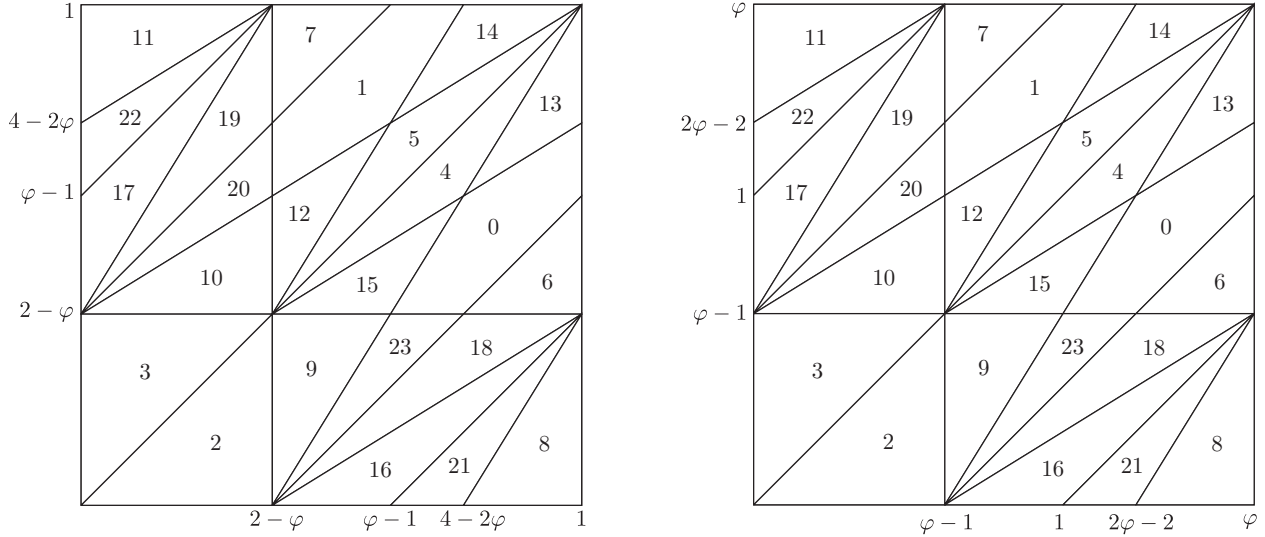


FIGURE 8. The partition deduced from the dot pattern of Figure 7 is at left. At right, this partition is scaled by a factor of φ , giving us partition \mathcal{P}_{24} , which makes the formula for the \mathbb{Z}^2 action R_{24} on the partitioned torus simpler. The slopes of lines in the partition are $0, 1, \infty, \varphi$, and $1/\varphi$.

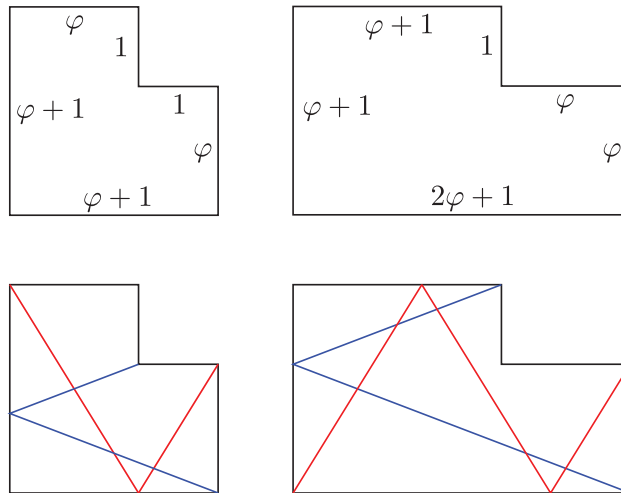


FIGURE 9. The Ammann A2 order-2 aperiodic protset. The top row shows the dimensions of the two tiles (φ is the golden mean), and on the bottom row, the tiles are adorned with decorations called *Ammann bars* that indicate the matching rules that enforce aperiodicity for A2.

valid tilings. In doing so, we will consider orbits of points on the torus that intersect the boundary and points whose orbits do not.

Let $\mathbf{T} = [0, \varphi] \times [0, \varphi]$ where \mathbf{T} has partition \mathcal{P}_{24} and let $p = (0.1, 0.2) \in \mathbf{T}$. We then consider the orbit $\mathcal{O}_{R_{24}}(p) \subset \mathbf{T}$. We wish to see if the tiling (or at least a finite portion we can generate) spelled out by $\mathcal{O}_{R_{24}}(p)$ seems to be valid. This process could be automated, but we will do it “by hand”, drawing the orbit in Figure 15 and the corresponding partial configuration in Figure 16. Notice that the partial tiling so generated is valid. Also note that we could easily convert the Wang tiling of Figure 16 into a tiling by the Penrose rhombs (P3) simply by substituting the patches described in Figure 5 for the corresponding Wang tiles. Similarly, in Figure 17 we see part of the

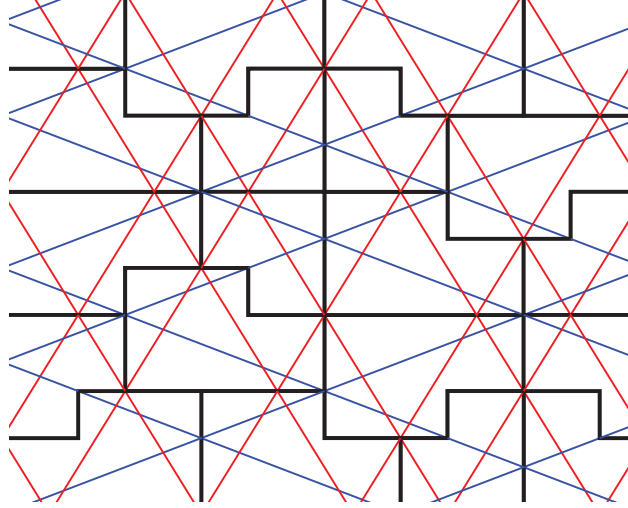


FIGURE 10. A patch of tiling formed from the A2 prototile

1	3	4	6	4	6	3	3
1 0 2	3 1 4	4 2 5	6 3 3	3 4 5	3 5 3	4 6 4	6 7 4
2	4	5	3	4	4	5	3
5	4	5	3	2	2	2	1
2 8 1	2 9 1	1 10 1	2 11 2	4 12 6	5 13 3	3 14 6	5 15 4
3	6	4	6	1	1	2	1

 FIGURE 11. The order-16 aperiodic Wang tile prototile, \mathcal{T}_{16} , derived from the A2 prototile.

orbit $\mathcal{O}_{R_{16}}(p)$ of the point $p = (0.1, 0, 1)$ in the torus \mathbf{T} partitioned by \mathcal{P}_{16} the corresponding partial tiling by the order-16 Ammann Wang tiles (\mathcal{T}_{16}) in 18, which again appears to be valid.

It is not hard to check that the orbit of any point $p \in \mathbf{T}$, under either action R_{24} or R_{16} , will be dense in \mathcal{T} . Thus, one immediate consequence of $\mathcal{X}_{\mathcal{P}_{24}, R_{24}}$ and $\mathcal{X}_{\mathcal{P}_{16}, R_{16}}$ being subspaces of Ω_{24} and Ω_{16} (respectively) is that the areas of atoms in \mathcal{P}_{24} and \mathcal{P}_{16} correspond to the proportion of tiles of specific kinds in tilings. For example, the area of the atom labeled 0 in \mathcal{P}_{16} (Figure 14) is $(\varphi - 1)^2 = 2 - \varphi$, which comprises $(2 - \varphi)/\varphi^2 = 5 - 3\varphi \approx 14.59\%$ of the area of the torus \mathbf{T} . This means that in any tiling in $\mathcal{X}_{\mathcal{P}_{16}, R_{16}}$, about 14.59% of the tiles will be copies of the prototile T_0 .

4.4. Orbits that intersect the boundary of \mathcal{P} . Let Δ_{16} be the union of the boundary lines of the atoms in \mathcal{P}_{16} . In this subsection we consider an example where the orbit of a point in \mathcal{T} intersects Δ_{16} , and we note that the details are similar in \mathcal{P}_{24} . We will illustrate by example how the ambiguity that arises in assigning tiles to points in the orbit on Δ_{16} is resolved and we will see a certain interesting phenomenon in the dynamics of $\mathcal{X}_{\mathcal{P}, R}$.

Let $p = \mathbf{0} = (0, 0) \in \mathbf{T}$ and let $q = (1/2, (3/2)\varphi - 1) \in \mathbf{T}$. Notice that p lies at the intersection of lines of all 4 slopes of boundary lines in \mathcal{P} since this torus \mathbf{T} is formed as a quotient by identifying opposite sides. Also notice that q lies on a boundary segment of slope φ connecting $(0, \varphi - 1)$ and $(\varphi - 1, 1)$. Consider the orbit $\mathcal{O}_{R_{16}}(p)$. Using the computer, inside of a finite window of size $[-40, 40] \times [-40, 40]$, we can check which points $\mathbf{n} \in \mathbb{Z}^2$ satisfy $R_{16}^{\mathbf{n}}(\mathbf{0}) \pmod{\mathbf{T}} \in \Delta_{16}$, and a plot of these points \mathbf{n} is shown in Figure 19a. Similarly, inside the same size window, we plot the points $\mathbf{n} \in \mathbb{Z}^2$ satisfying $R_{16}^{\mathbf{n}}(q) \pmod{\mathbf{T}} \in \Delta_{16}$ in Figure 19b. Interestingly, we find that the points $\mathbf{n} \in \mathbb{Z}^2$ where the orbit falls on the boundary forms straight strips of points, sometimes a single strip (when the orbit touches lines in the boundary of just one slope) or four separate strips

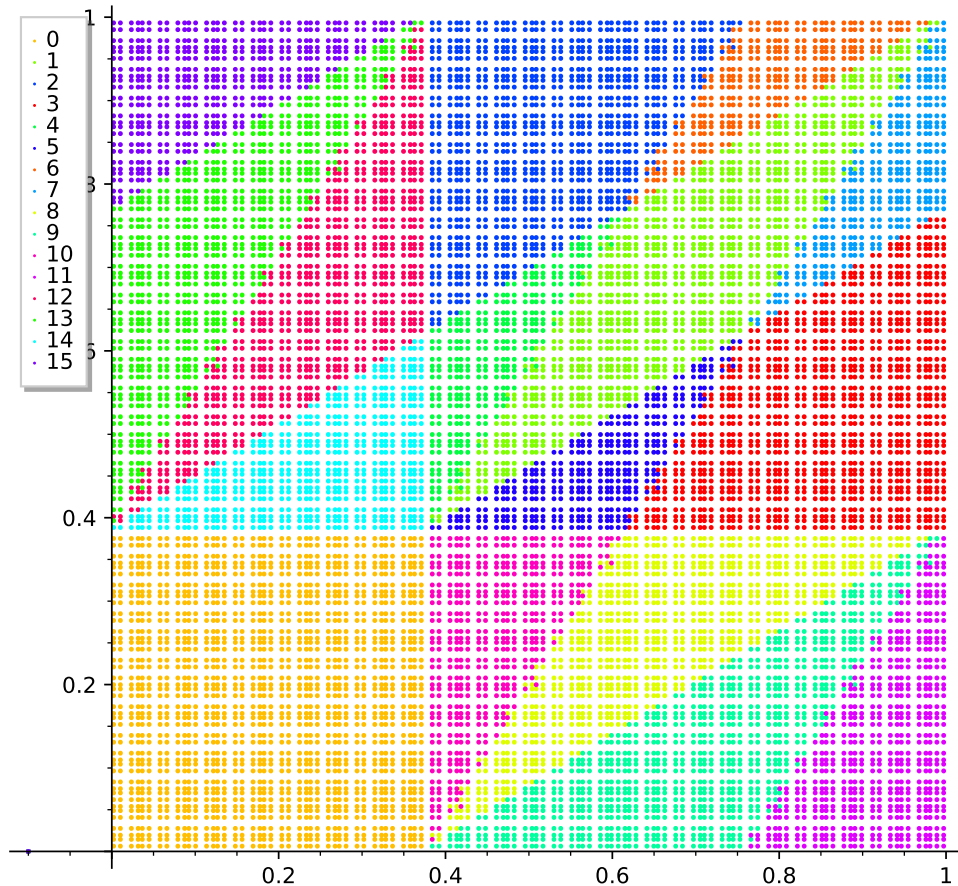


FIGURE 12. The dot pattern produced by applying matrix A_{16} to a 120×120 patch of tiling by the order-16 Wang tile protoset derived from the Ammann A2 aperiodic protoset.

(when the orbit touches lines in the boundary of different slopes). The directions of the strips are called the *nonexpansive directions* of $\mathcal{X}_{\mathcal{P}_{16}, R_{16}}$. In [LMM22], the authors provide methodology for determining the exact directions of such nonexpansive directions, and we leave that topic for the reader to explore further. We only mention here that these nonexpansive directions correspond to what are commonly called *Conway worms* in Penrose tilings [Gar97]; nonexpansive directions provides a very nice and more general explanation for such behavior in some tilings.

In either situation, the ambiguity in the corresponding tiling can be resolved by choosing a direction to determine what tile to place at the points \mathbf{n} such that $R_{16}^{\mathbf{n}}(p)$ lies on Δ_{16} . For example, if we again consider the orbit $\mathcal{O}_{R_{16}}(q)$ where q is as in Figure 19b, let us specify a direction vector $\mathbf{v} = (-1, 1)$. Notice that no line segment in Δ_{16} is parallel to \mathbf{v} . Now, at each point of \mathbf{n} where $\mathcal{O}_{R_{16}}(q)$ intersects Δ_{16} , place vector \mathbf{v} with its initial point at \mathbf{n} . Because \mathbf{v} is not parallel to any of the segments comprising Δ_{16} , then \mathbf{v} is pointing from \mathbf{n} into one of the atoms $P_i \in \mathcal{P}_{16}$. Thus, we can place a copy of prototile T_i at \mathbf{n} . The other choice is use $-\mathbf{v}$ to determine the choice of tile at each such point \mathbf{n} , which points toward the region on the opposite side of the boundary segment as does \mathbf{v} . This is illustrated in Figures 20 and 21.

5. CANDIDATE JEANDEL-RAO APERIODIC PROTOSETS

In [JR21], the authors provide 33 candidate order-11 aperiodic protosets; the computer algorithm that they used to find the aperiodic set \mathcal{T}_0 could not rule out these 33 candidate sets as ones that

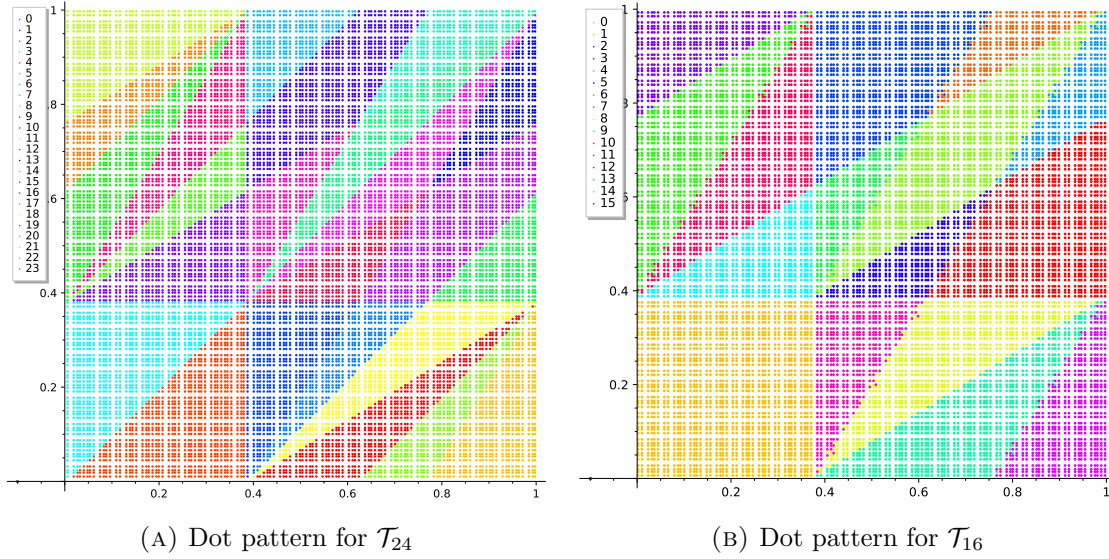


FIGURE 13. The dot patterns for \mathcal{T}_{24} and \mathcal{T}_{16} are remarkably similar; the pattern for \mathcal{T}_{16} can be obtained from the one for \mathcal{T}_{24} by removing the lines of slope 1.

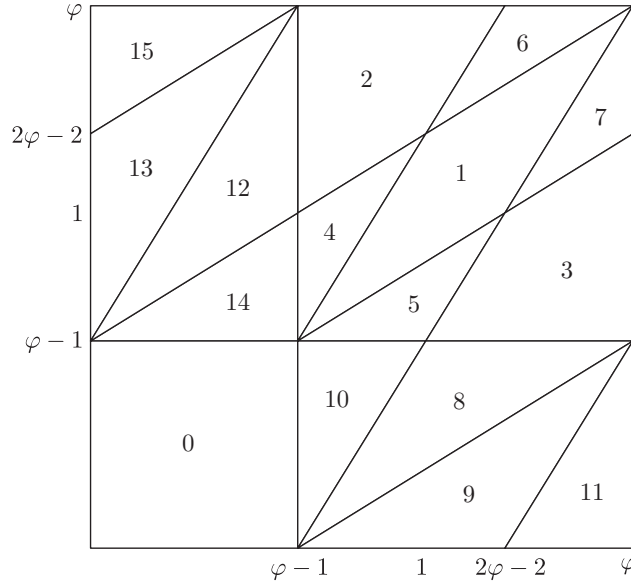


FIGURE 14. The partition \mathcal{P}_{16} obtained from the order-16 protoset \mathcal{T}_{16} .

admit periodic tilings, so it is likely that they are aperiodic protosets. In any event, as a matter of investigation, we will consider one of these candidate sets as an example. This set, depicted in Figure 22, we will call \mathcal{T}_2 .

We find that the lattice Γ_0 associated with the original Jeandel-Rao aperiodic protoset does not resolve a coherent dot pattern. However, a variation of Γ_0 does: Define Γ_2 to be the lattice in \mathbb{R}^2 generated by the vectors $(p, 0)$ and $(2 - p, p + 3)$. We see that Γ_2 does succeed in resolving a clear dot pattern, shown in Figure 23. Noticing that this dot pattern is very similar to the partition \mathcal{P}_0 , it is not hard to arrive at a precise partition \mathcal{P}_2 for \mathcal{T}_2 , which is shown in Figure 24. Finally, it appears, at least experimentally, that using the \mathbb{Z}^2 action $R_2^n(p) = p + \mathbf{n} \pmod{\Gamma_2}$ defined on the torus $\mathbf{T}_2 = [0, \varphi] \times [0, \varphi + 3]$ that is endowed with the partition \mathcal{P}_2 , produces valid tilings (see figure

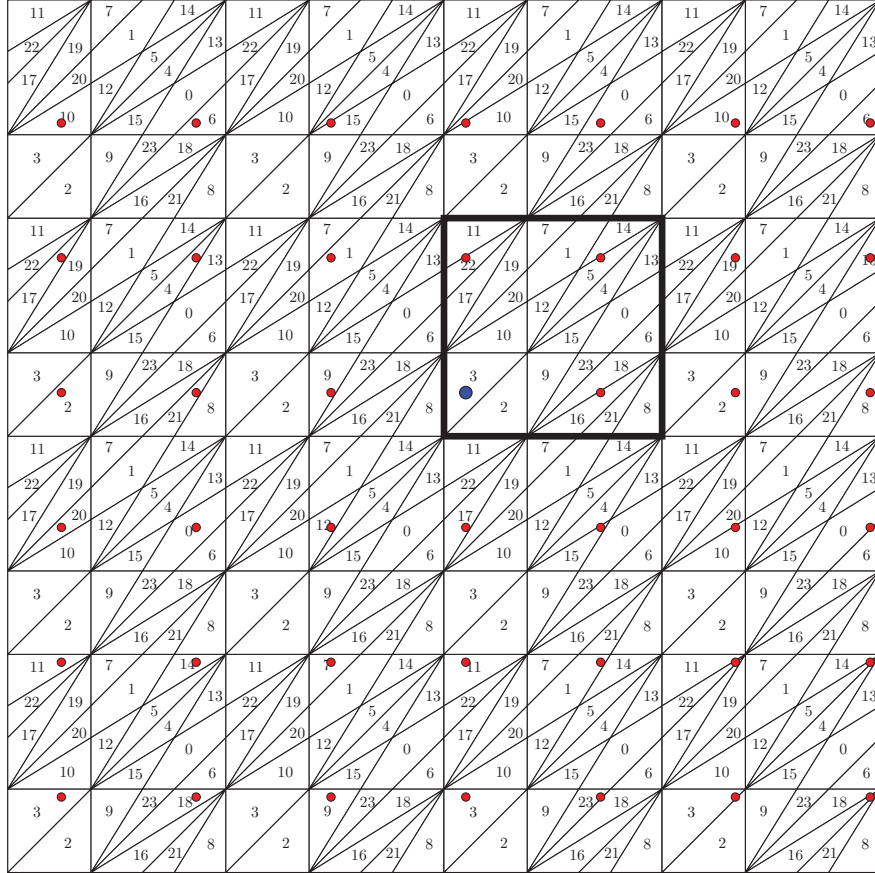


FIGURE 15. The orbit of the point $p = (0.1, 0.2)$ under the action R_{24} in the torus $\mathbf{T} = [0, \varphi] \times [0, \varphi]$ where \mathbf{T} has the partition \mathcal{P}_{24} . The point p is in blue, and the rest of its orbit is in red.

25). Perhaps an analysis of the dynamical systems properties of $\mathcal{X}_{\mathcal{P}_2, R_2}$ can be leveraged to argue that the full Wang shift Ω_2 is aperiodic or has other interesting properties.

6. IDENTIFYING THE SIGNATURE OF THE UNDERLYING LATTICE

Here we discuss some methodology for determining the lattices for Wang shifts such as Ω_0 , Ω_{16} , Ω_{24} and Ω_2 . Let \mathcal{T} be some protoset of Wang tiles, and suppose that there is a hidden encoding of tilings in $\Omega_{\mathcal{T}}$ via a \mathbb{Z}^2 action on a partitioned torus, as with the Wang shifts discussed above. Then there is a lattice Γ generated by vectors γ_1 and γ_2 giving rise to a torus $\mathbf{T} = \mathbb{R}^2/\Gamma$, along with a \mathbb{Z}^2 action R on \mathbf{T} defined by $R^n(x) = x + \mathbf{n} \pmod{\Gamma}$, and there is a topological partition $\mathcal{P} = \{P_0, P_1, \dots, P_{n-1}\}$ of \mathcal{T} used to encode the orbits of points in \mathcal{T} under R as tilings.

When we look at a tiling in $\Omega_{\mathcal{T}}$, we may notice the repeating patterns within the tiling that suggest “golden” rotations are responsible for the patterns. Such rotations have some signature behavior, such as having “near periods” of length approximately equal to Fibonacci numbers and encoding infinite patterns that are in correspondence with the Fibonacci word. An example of such a golden rotation is a 1-dimensional \mathbb{Z} action (rotation) R_φ of the unit interval $[0, \varphi + 1]$ defined by $R_\varphi^n(x) = x + n \pmod{\varphi + 1}$. We partition $[0, \varphi + 1]$ into two subintervals $P_0 = (0, \varphi)$ and $P_1 = (\varphi, \varphi + 1)$. We can use the action R_φ and the partition $\mathcal{P} = \{P_0, P_1\}$ to encode points in $[0, \varphi]$ as bi-infinite sequences as follows: For each $x \in [0, \varphi + 1]$ and $n \in \mathbb{Z}$, if $R^n(x) \in P_0 \cup \{0\}$, we place 0 at the n -th decimal place of a binary decimal expansion, and if $R^n(x) \in P_1 \cup \{\varphi\}$, we place 1 at the n -th decimal place. For example, if we encode $0 \in [0, \varphi]$ according to this scheme, we get

18	1	1	18	1	18	1
9 10 4 4	6 15	15 15 9 9	9 10 4 4	0 9	9 10 4 4	6 15
8	14	6	8	5	8	14
8	14	6	8	5	8	14
3 17 15 15	4 10	10 1 3 3	22 9 9	5 16	16 19 4 4	13 10
7	6	2	18	13	7	5
7	6	2	18	13	7	5
12 2 17 17	21 12	12 9 17	17 3 11	11 16 12	12 2 17 17	8 11
18	1	6	8	1	18	1
18	1	6	8	14	18	1
10 20 4 4	0 9 9	12 3 3	17 15 15	4 10	10 20 4 4	0 9
7	5	13	7	6	7	5
7	5	13	7	6	8	5
3 11 10 10	14 16	16 7 3 3	11 10 10	1 3 3	22 9 9	5 16
18	2	2	18	2	18	13
18	2	2	18	2	18	13
17 3 11 11	18 12	12 9 17	17 3 11 11	23 17	17 3 11 11	16 12
8	14	6	8	5	8	1

FIGURE 16. The \mathcal{T}_{24} tiling corresponding to the orbit $\mathcal{O}_{R_{24}}((0.1, 0.2))$ shown in Figure 15. The blue tile corresponds to the point $(0.1, 0.2)$.

the bi-infinite binary decimal expansion

$$\dots 01001010010010100101.001001010010010100101\dots,$$

which is the well-known Fibonacci word. The presense of repeating patterns in a tiling along a line that follow the pattern of a Fibonacci word suggests that the toral rotation in the direction of that line is something akin to R_φ .

Another signature is the spacing of repeating structures. Going back to R_φ , consider the orbit $\mathcal{O}_{R_\varphi}(x)$ of some point $x \in [0, \varphi + 1]$. It is not hard to check that $\mathcal{O}_{R_\varphi}(x)$ is dense in $[0, \varphi + 1]$. Thus, there are many values of $n \in \mathbb{Z}$ such that $R^n(x) \approx x$. For what values of n is $R^n(x) \approx x$? It turns out that when $|n|$ is a Fibonacci number, we see that $R^n(x) \approx x$. This is a result of a property of the Fibonacci sequence $(F_n) = (1, 1, 2, 3, 5, 8, \dots)$ which has the well-known property that $F_{n+1}/F_n \rightarrow \varphi$ as $n \rightarrow \infty$. From this limit, we see that a Fibonacci number (which is integer valued) is approximately a multiple of φ . Thus, we see that $R^n(x) = x + n \pmod{\varphi + 1} \approx x$ whenever $|n|$ is Fibonacci. The upshot here is that we expect to see repeating patterns within the encoding of x with spacing between these patterns being Fibonacci numbers.

Slightly generalizing the rotation R_φ , we may consider rotations $R_{(a,b)}$ of the interval $[0, a\varphi + b]$ ($a, b \in \mathbb{Z}$) defined by $R_{(a,b)}(x) = x + n \pmod{a\varphi + b}$. Whatever partition we place on $[0, a\varphi + b]$, in the encoding of $x \in [0, a\varphi + b]$ under $R_{(a,b)}$, we expect to see repeating patterns with spacing between these patterns being Fibonacci numbers because $R^n_{(a,b)}(x) = x + n \pmod{a\varphi + b} \approx x$ when $n \in \mathbb{Z}$ is approximately a multiple of $a\varphi + b$, which again happens when n is a multiple of $a\varphi$, which happens when n is a Fibonacci number. Thus, seeing a repeating pattern with gaps between being the size of Fibonacci numbers is suggestive of a rotation of the form $R_{(a,b)}$.

Now let us consider 2-dimensional \mathbb{Z}^2 toral rotations of a certain form: Suppose R is defined on a torus \mathbf{T} by $R^n(x) = x + \mathbf{n} \pmod{\Gamma}$ where $x \in \mathbf{T}$, $\mathbf{n} \in \mathbb{Z}^2$, and $\gamma_1 = (a\varphi + b, c\varphi + d)$ and $\gamma_2 = (e\varphi + f, g\varphi + h)$ ($a, b, c, d, e, f, g, h \in \mathbb{Z}$) are the generating vectors of the lattice Γ . If γ_1 is horizontal, then when R^n is restricted to those values of $\mathbf{n} = (n_1, n_2)$ where n_2 is fixed, R^n will behave like a golden rotation in the horizontal direction. Thus, to pick up the signature of horizontal golden rotation in a tiling, we look for repeating horizontal patterns in the tiling that

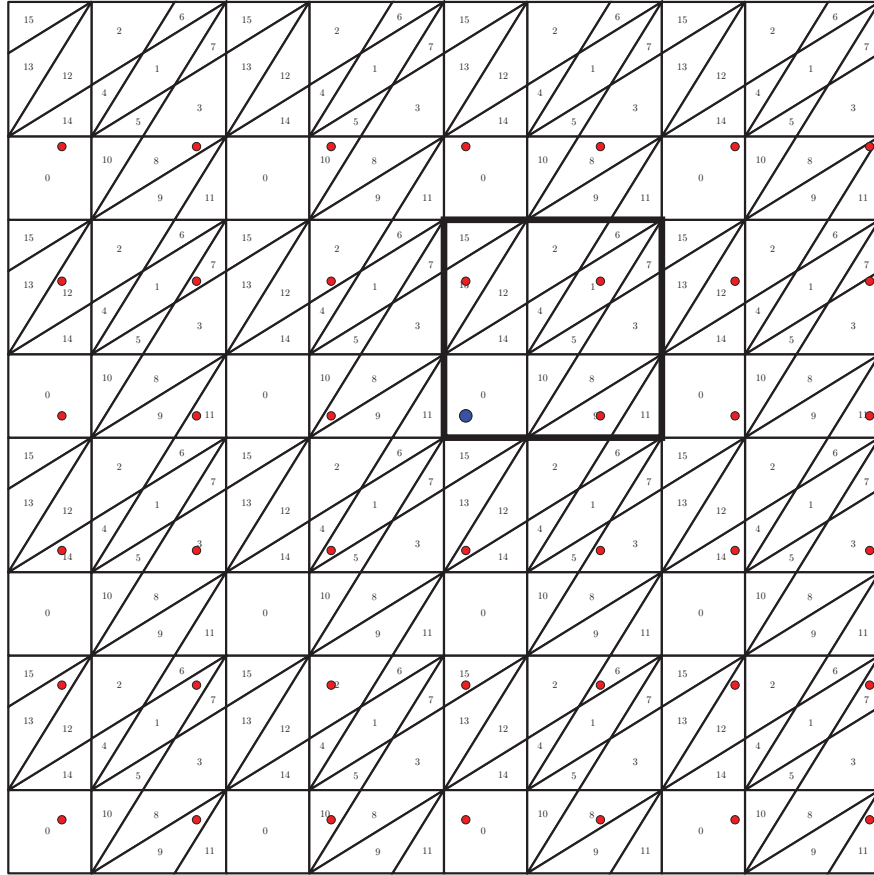


FIGURE 17. The orbit of the point $p = (0.1, 0.1)$ under the action R_{16} in the torus $\mathbf{T} = [0, \varphi] \times [0, \varphi]$ where \mathbf{T} has the partition \mathcal{P}_{16} . The point p is in blue, and the rest of its orbit is in red.

have spacing between these patterns being Fibonacci numbers. A similar thing could happen in the vertical direction or any slant direction; in a slant direction, we would look for a repeating pattern with spacing that is a Fibonacci number multiple of a vector parallel to that direction.

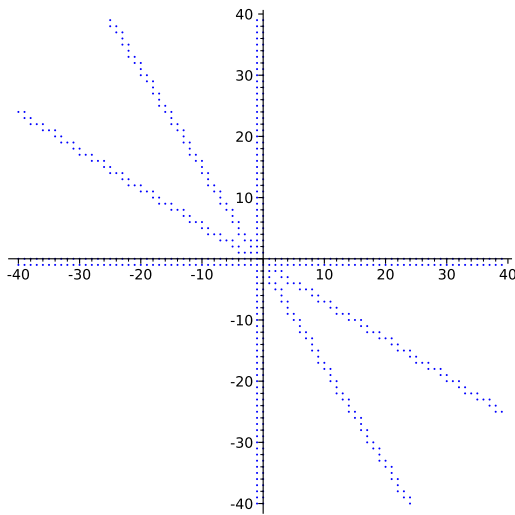
While spotting the tell-tale behavior of a golden rotation in a direction inside a tiling is not too difficult to do, finding this direction is of the form $(a\varphi + b, c\varphi + d)$ and finding the specific values of a, b, c , and d are two different questions. We have not yet discovered a way to pinpoint these values from properties of the tiling, but it is not too hard to have the computer test values of a, b, c , and d over a range of integers, say where each variable ranges over integers between -3 and 3 , and see if any of those values produce dot patterns indicating clear partitions. And this is exactly what one can do to find dot patterns for the partitions \mathcal{P}_0 , \mathcal{P}_2 , \mathcal{P}_{16} , and \mathcal{P}_{24} .

As an example, consider the computer generated partial tiling admitted by \mathcal{T}_{16} (the Wang tile version of the Ammann A2 protoset) shown in Figure 26. Tile 15 has been colored to make it stand out in contrast to the other tiles of the tiling. One notices the signatures of golden rotations within this tiling in both the horizontal and vertical directions - See Figure 26. This is suggestive of golden toral rotations in vertical and horizontal directions of the form $(a\varphi + b, 0)$ and $(0, c\varphi + d)$, and luckily, the simplest vectors $\gamma_1 = (\varphi, 0)$ and $\gamma_2 = (0, \varphi)$ produce a nicely resolved dot pattern from which we determined the partition \mathcal{P}_{16} for \mathcal{T}_{16} .

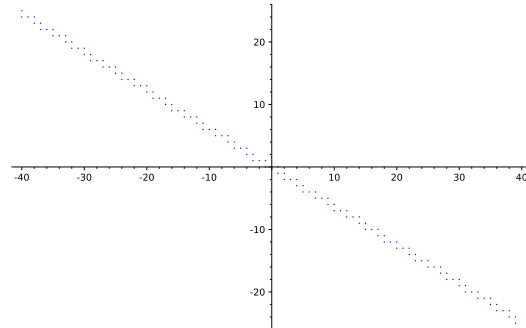
Other tilings exhibiting golden rotations do not give up their secret lattices quite as easily. For example, in Figure 27, we give a portion of a tiling admitted by the Jeandel-Rao candidate aperiodic protoset \mathcal{T}_2 . Using the computer to find clearly resolved dot patterns turned up a few essentially

	1	5	5	1	5	1	4													
1	0	2	2	8	1	1	10	1	1	0	2	2	8	1	1	0	2	2	9	1
	2	3	4	2	3	2	6													
2	3	4	4	2	5	5	13	3	3	1	4	4	12	6	6	3	3			
	1	3	5	1	4	1	3													
1	0	2	2	11	2	2	8	1	1	0	2	2	9	1	1	0	2	2	11	2
	2	6	3	2	6	2	6													
2	6	3	3	1	4	4	12	6	6	3	3	3	14	6	6	3	3			
	2	3	4	1	3	2	3													
2	3	4	4	3	2	3														
5	13	3	3	1	4	4	2	5	5	15	4	4	6	4	4	12	6	6	7	4
	1	4	5	1	5	1	3													
1	0	2	2	9	1	1	10	1	1	0	2	2	8	1	1	0	2	2	11	2
	2	6	4	2	3	2	6													

FIGURE 18. The \mathcal{T}_{16} tiling corresponding to the orbit $\mathcal{O}_{R_{16}}((0.1, 0.1))$ shown in Figure 17. The blue tile corresponds to the point $(0.1, 0.1)$.



(A) Points \mathbf{n} such that $R_{16}^{\mathbf{n}}(\mathbf{0}) \in \Delta_{16}$



(B) Points \mathbf{n} such that $R_{16}^{\mathbf{n}}(\mathbf{q}) \in \Delta_{16}$, where $q = (1/2, (3/2)\varphi - 1)$.

FIGURE 19. When orbits of points that intersect Δ_{16}

equivalent possibilities, one of which is depicted in Figure 23. The golden rotational behavior (Fibonacci spacing) corresponding to the two vectors generating that dot pattern is illustrated in Figure 27.

We conclude this section by giving a snippet of code that show how we found the lattice vectors for \mathcal{T}_2 that produced a clearly resolved dot pattern, revealing the underlying partition.

```

1 from slabbe import WangTileSet
2 import itertools
3

```

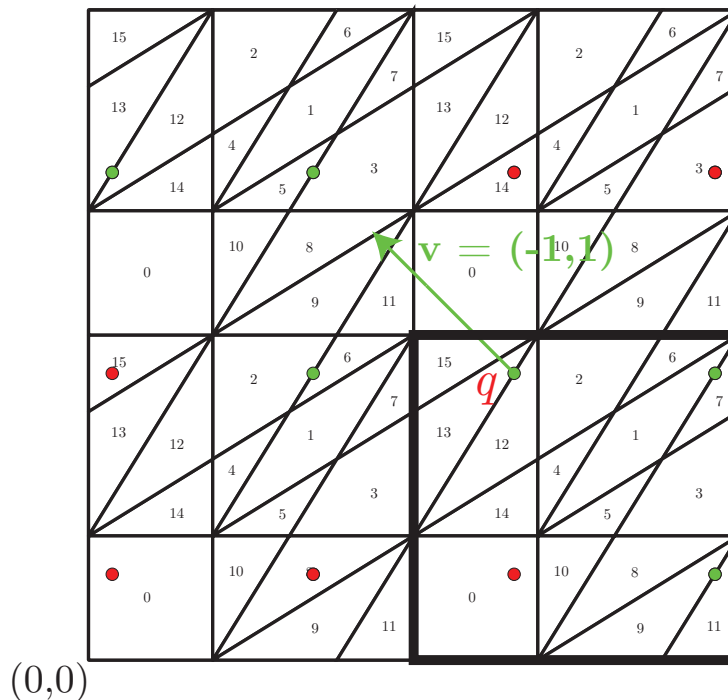


FIGURE 20. Using $\mathbf{v} = (-1, 1)$ (in green) to resolve the tiles corresponding to points on Δ_{16} . At $q = (1/2, (3/2)\varphi - 1)$, \mathbf{v} points to region 13 and $-\mathbf{v}$ points to region 12. The point q corresponds to the tiles shaded red in Figure 21.

4	2	3	2	3	4	2	3
4 2 5 5 13 3 3 1 4 4 12 6 6 7 4 4 2 5 5 13 3 3 1 4							
5	1	4	1	3	5	1	4
5	1	4	1	3	5	1	4
1 10 1 1 0 2 2 9 1 1 0 2 2 11 2 2 8 1 1 0 2 2 9 1							
4	2	6	2	6	3	2	6
4	2	6	2	6	3	2	6
3 4 5 5 13 3 3 5 3 3 14 6 6 3 3 3 1 4 4 12 6 6 3 3							
4	1	4	2	3	4	1	3
4	1	4	2	3	4	1	3
4 2 5 5 15 4 4 2 5 5 13 3 3 1 4 4 2 5 5 15 4 4 6 4							
5	1	5	1	4	5	1	5
5	1	5	1	4	5	1	5
1 10 1 1 0 2 2 8 1 1 0 2 2 9 1 1 10 1 1 0 2 2 8 1							
4	2	3	2	6	4	2	3
4	2	3	2	6	4	2	3
3 4 5 5 13 3 3 1 4 4 12 6 6 3 3 3 4 5 5 13 3 3 1 4							
4	1	4	1	3	4	1	4
4	1	4	1	3	4	1	4
2 9 1 1 0 2 2 9 1 1 0 2 2 11 2 2 9 1 1 0 2 2 9 1							
6	2	6	2	6	6	2	6
6	2	6	2	6	6	2	6
3 5 3 3 14 6 6 3 3 3 14 6 6 3 3 3 5 3 3 14 6 6 3 3							
4	2	3	2	3	4	2	3

(A) Using $\mathbf{v} = (-1, 1)$ to resolve the tiles corresponding to points on Δ_{16} .

4	2	3	2	3	4	2	3
4 2 5 5 13 3 3 1 4 4 12 6 6 7 4 4 2 5 5 13 3 3 1 4							
5	1	4	1	3	5	1	4
5	1	4	1	3	5	1	4
2 8 1 1 0 2 2 9 1 1 0 2 2 11 2 2 8 1 1 0 2 2 9 1							
3	2	6	2	6	3	2	6
3	2	6	2	6	3	2	6
3 1 4 4 12 6 6 3 3 3 14 6 6 3 3 3 1 4 4 12 6 6 3 3							
4	1	3	2	3	4	1	3
4	1	3	2	3	4	1	3
4 2 5 5 15 4 4 6 4 4 12 6 6 7 4 4 2 5 5 15 4 4 6 4							
5	1	5	1	3	5	1	5
5	1	5	1	3	5	1	5
1 10 1 1 0 2 2 8 1 1 0 2 2 11 2 2 8 1 1 0 2 2 8 1							
4	2	3	2	6	3	2	3
4	2	3	2	6	3	2	3
3 4 5 5 13 3 3 1 4 4 12 6 6 3 3 3 1 4 4 12 6 6 7 4							
4	1	4	1	3	4	1	3
4	1	4	1	3	4	1	3
2 9 1 1 0 2 2 9 1 1 0 2 2 11 2 2 9 1 1 0 2 2 11 2							
6	2	6	2	6	6	2	6
6	2	6	2	6	6	2	6
3 5 3 3 14 6 6 3 3 3 14 6 6 3 3 3 5 3 3 14 6 6 3 3							
4	2	3	2	3	4	2	3

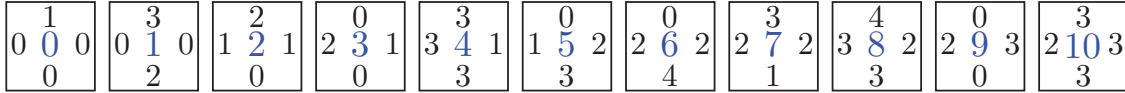
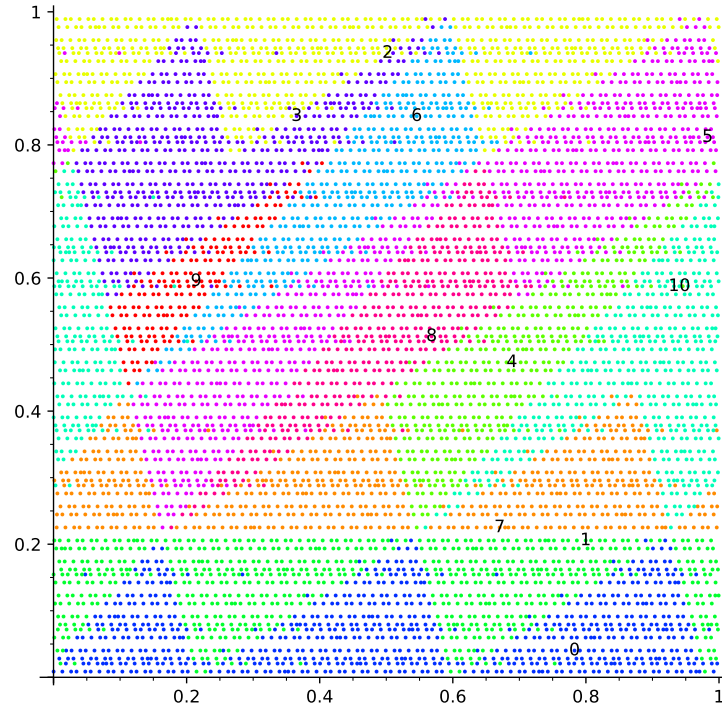
(B) Using $-\mathbf{v} = (1, -1)$ to resolve the tiles corresponding to points on Δ_{16} .

FIGURE 21. Two tilings that are the same except at the colored tiles, which correspond to points \mathbf{n} where the orbit of a point intersects Δ_{16} . The tiles in red correspond to the point $q = (1/2, (3/2)\varphi - 1)$ in Figure 20.

```

4 #Creating the Wang tiles
5 T2_tiles = [(0,1,0,0), (0,3,0,2), (1,2,1,0), (1,0,2,0), (1,3,3,3), (2,0,1,3), (2,0,2,4)
, (2,3,2,1), (2,4,3,3), (3,0,2,0), (3,3,2,3)]

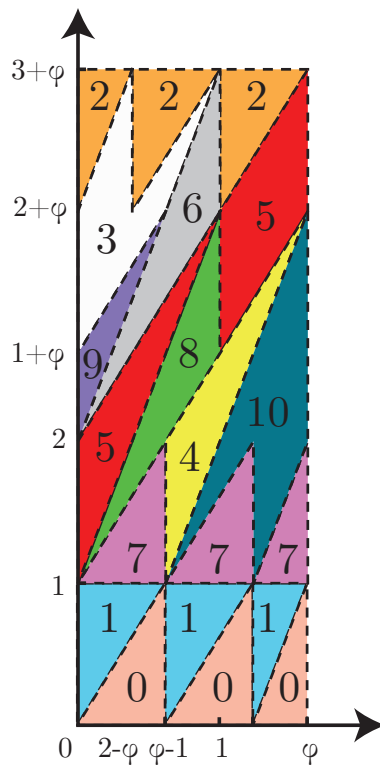
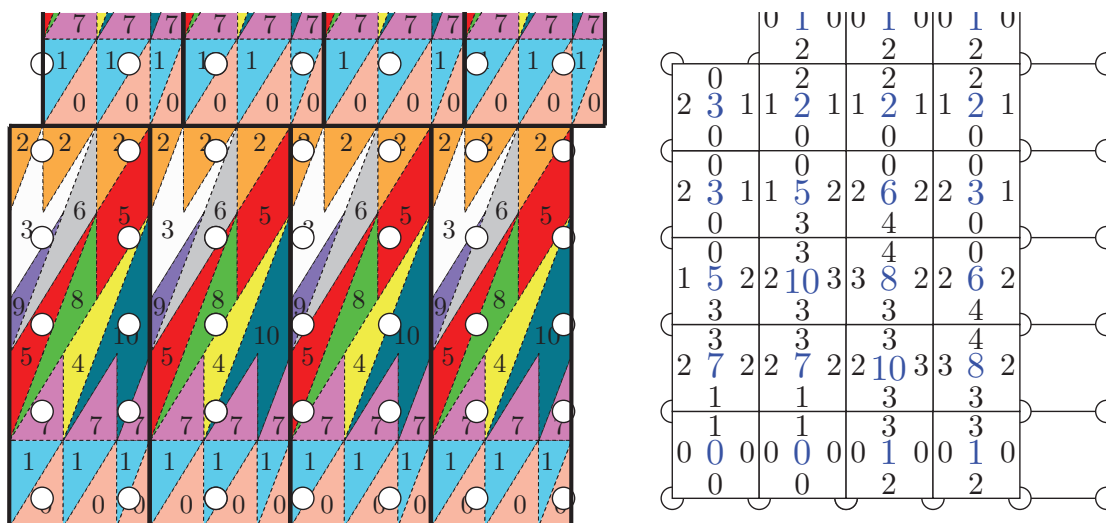
```

FIGURE 22. Jeandel-Rao candidate aperiodic protoset \mathcal{T}_2 .FIGURE 23. A dot pattern found by applying matrix $\begin{pmatrix} \varphi & 2-\varphi \\ 0 & \varphi+3 \end{pmatrix}^{-1}$ to a large patch of tiling by \mathcal{T}_2 .

```

6 T2 = WangTileSet(T2_tiles)
7
8 #Generating a large patch of tiling with bottom row all copies of tile 6
9 preassigned_tiles = {(a,0):6 for a in range(100)};
10 S2 = T2.solver(100,62,preassigned_tiles=preassigned_tiles);
11 T2_tiling = S2.solve(solver='glucose');
12
13 #Coloring all copies of tile 10 yellow in the tiling
14 positions = T2_tiling.tile_positions([10])
15 extra = []
16     for (x,y) in positions:
17         extra.append(r'\draw[fill=yellow]({},{})rectangle({},{});'.format(x,y,x+1,
18             y+1))
19 extra = '\n'.join(extra)
20
21 #Displaying the tiling with and without the colored copies of tile 10
22 T2s.tikz()
23 T2_tiling.tikz(extra_before=extra)
24
25 #Testing a range of lattice generators (columns of M)

```

FIGURE 24. A partition for \mathcal{T}_2 .

z

FIGURE 25. Orbits of points in \mathbf{T}_2 partitioned with \mathcal{P}_2 under the action R_2 seem to produce valid tilings. The reader is encouraged to produce the next two columns of the tiling at right!

```

25 #to see if they resolve a clear dot pattern for a partition
26 for P in itertools.product([-1,0,1],[0,1,2],[0,1,2],[0,1,2],[0,1,2,3]):
27 M = matrix.column([[p+P[0],0],[P[1]*p+P[2],P[3]*p+P[4]]]);
28 if M.determinant() != 0:

```

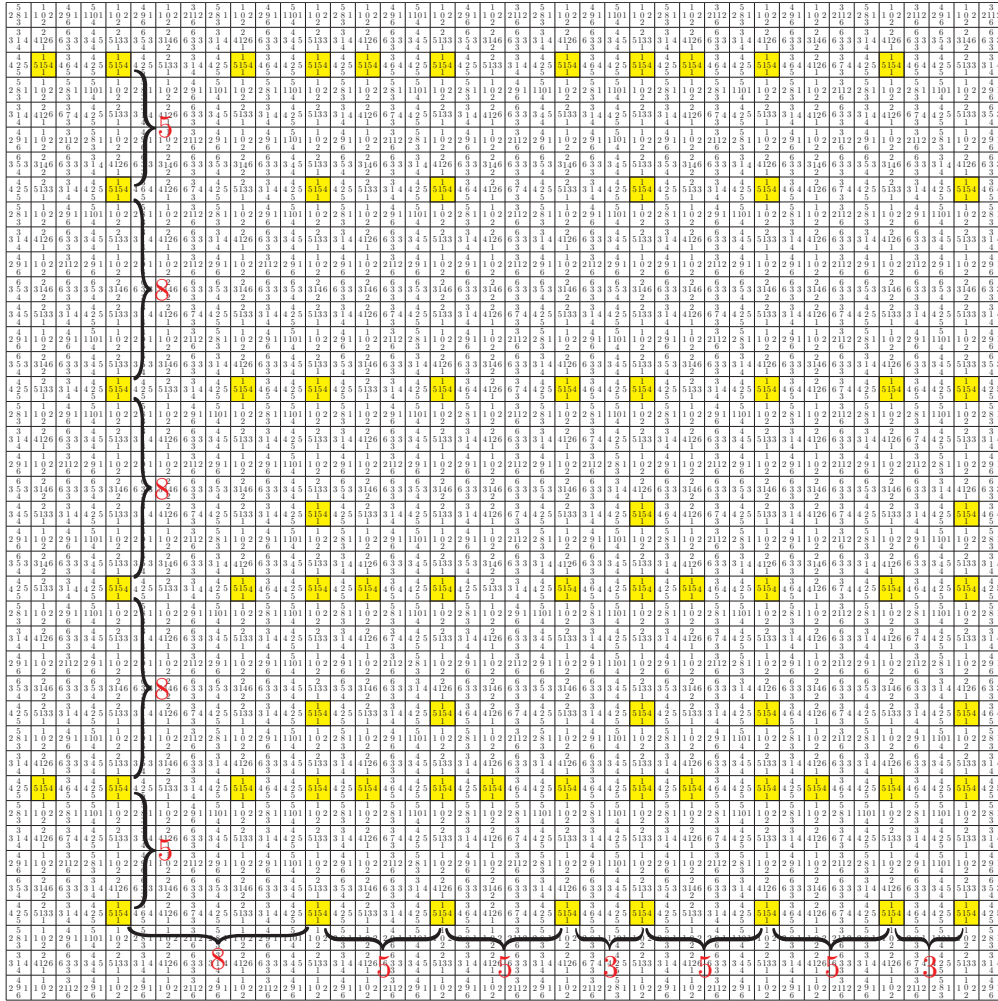


FIGURE 26. A partial tiling by \mathcal{T}_{16} exhibiting evidence of golden toral rotations. Tile T_{15} is colored yellow.

```

29 print(P)
30 T2_tiling.plot_points_on_torus(M.inverse()).show()

```

ACKNOWLEDGEMENTS

The authors would like to thank Sébastien Labbé for his helpful suggestions.

Appendices

A. DYNAMICAL SYSTEMS AND WANG TILINGS

Here we will give a little deeper into the Labbé's theory, given more definitions and citing several theorems, then applying it to prove some facts about $\mathcal{X}_{\mathcal{P}_{16}, R_{16}}$. First, we provide some additional details and definitions, following the ideas laid out in [Lab21].

Recall from Subsection 2.1 that a topological dynamical system is a triple (X, G, S) where X is a topological space, G is a topological group, and S is a continuous function $S: G \times X \rightarrow X$ which defines a left action of G on X . For $A \subseteq X$, we will use \overline{A} to indicate the *topological closure*

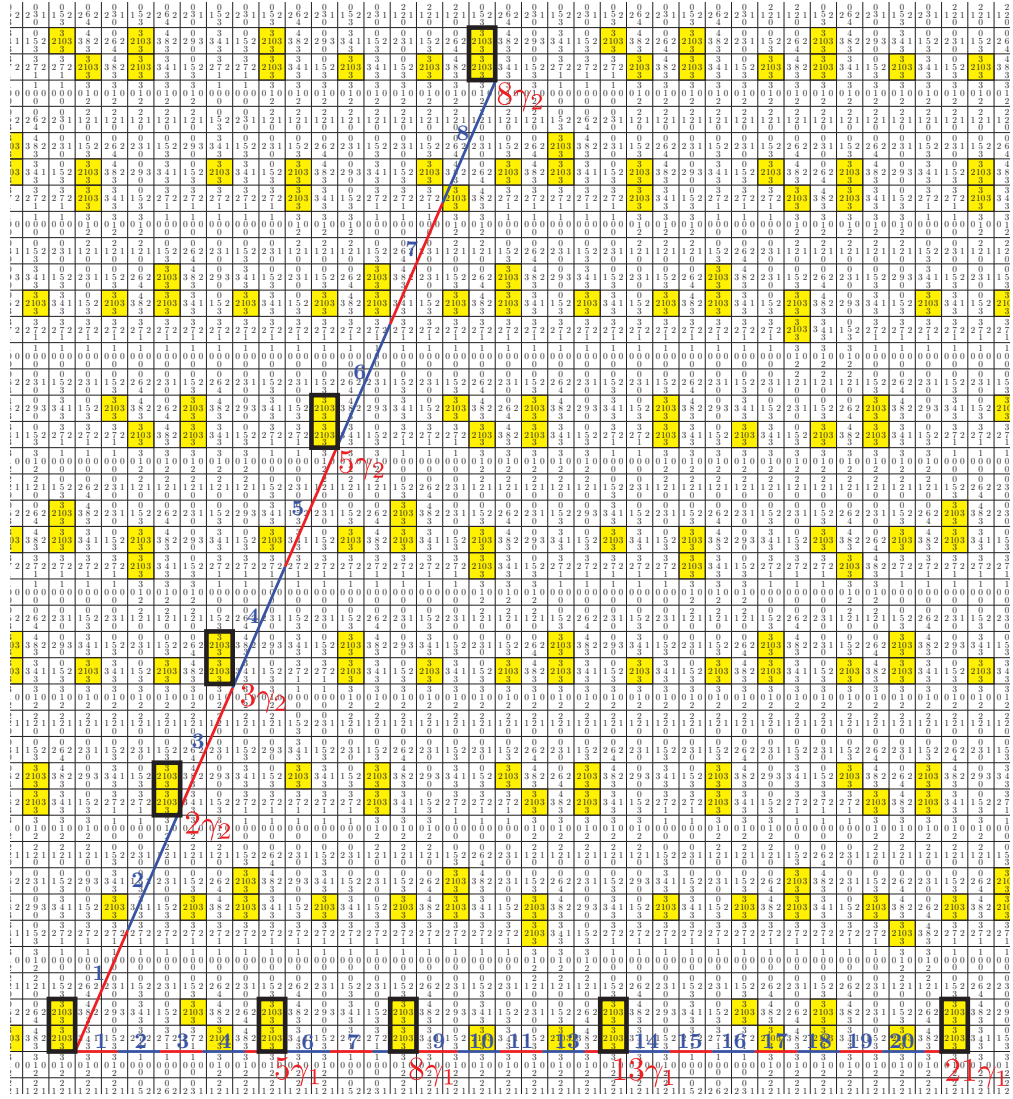


FIGURE 27. A partial tiling by \mathcal{T}_2 exhibiting evidence of golden toral rotations. γ_1 and γ_2 are vectors generating a lattice that resolves the tiling to a clear dot pattern as seen in Figure 12. Tile T_{10} is colored yellow.

d

of A in X . We also define another kind of closure - the S -closure - by $S(A) = \cup_{g \in G} S^g(A)$, and we will say that A is S -invariant if $S(A) = A$. We say the system (X, G, S) is *minimal* if X contains no proper, nonempty, (topologically) closed, S -invariant subsets.

Recall from Subsection 2.1 that the configuration space, $\mathcal{T}^{\mathbb{Z}^2}$, where \mathcal{T} is a Wang tile protoset, is thought of as the space of all possible tilings (valid and nonvalid) of the plane by \mathcal{T} . The configuration space $\mathcal{T}^{\mathbb{Z}^2}$ is a topological space when endowed with the compact product topology, and moreover, this topology is generated by the metric d on $\mathcal{T}^{\mathbb{Z}^2}$ defined by $d(x, x') = 1/2^{\min\{\|\mathbf{n}\| \in \mathbb{Z}^2 : x_{\mathbf{n}} \neq x'_{\mathbf{n}}\}}$. In the formula for this metric, $\min\{\|\mathbf{n}\| \in \mathbb{Z}^2 : x_{\mathbf{n}} \neq x'_{\mathbf{n}}\}$ is a value of \mathbf{n} closest to the origin where x and x' do not agree, so $d(x, x')$ is close to 0 when x and x' agree on a large patch centered at the origin, and $d(x, x')$ is close to 1 when x and x' disagree near the origin. $(\mathcal{T}^{\mathbb{Z}^2}, \mathbb{Z}^2, \sigma)$, where σ is the shift action, is a topological dynamical system, and in this particular setting, if $X \subseteq \mathcal{T}^{\mathbb{Z}^2}$ is σ -invariant, we say X is *shift-invariant*. For a space of Wang tilings X (say, a space of Wang tilings admitted by a protoset, or a space of tilings having some defining property), shift-invariance

is clearly a desirable property, for if $x' = \sigma(x)$ where $x \in X$, that just means x' is a translation of x , so x and x' are really the same tilings, and thus, we would want X to contain both. If X is topologically closed and shift invariant in $\mathcal{T}^{\mathbb{Z}^2}$, then we call X a **subshift** of $\mathcal{T}^{\mathbb{Z}^2}$. Notice that $(X, \mathbb{Z}^2, \sigma)$ is a topological dynamical system when X is a subshift of $\mathcal{T}^{\mathbb{Z}^2}$.

A.1. Shifts of Finite Type. Of particular importance in the context of tilings are *shifts of finite type*. A subshift of Wang tilings X being a shift of finite type essentially means, informally, that the tilings in X are completely determined a set of forbidden arrangements of tiles, such as when two tiles cannot be placed adjacent to one another due to a mismatch in the edge matching rules. Formally, to define shift of finite type, for any finite subset $S \subseteq \mathcal{T}^{\mathbb{Z}^2}$, we define $\mathcal{T}^S = \{y: S \rightarrow \mathcal{T}\}$, and we call any element $p \in \mathcal{T}^S$ a **pattern**. Next, we define the projection map $\pi_S: \mathcal{T}^{\mathbb{Z}^2} \rightarrow \mathcal{T}^S$ which restricts any configuration $x \in \mathcal{T}^{\mathbb{Z}^2}$ to S (i.e. $\pi_S(x) = x|_S$). We say $X \subseteq \mathcal{T}^{\mathbb{Z}^2}$ is a **shift of finite type (SFT)** if there exists a finite set of patterns \mathcal{F} called **forbidden patterns** such that

$$X = \{x \in \mathcal{T}^{\mathbb{Z}^2} \mid \pi_S \circ \sigma^{\mathbf{n}}(x) \notin \mathcal{F} \ \forall \mathbf{n} \in \mathbb{Z}^2, S \subset \mathbb{Z}^2\}.$$

It is clear that the full Wang shift $\Omega_{\mathcal{T}}$ of a protoset of Wang tiles \mathcal{T} is an SFT - the set of finite set forbidden patterns is formed simply as a set of representative invalid horizontal and vertical pairings of tiles from the protoset. However, for a subshift X of $\Omega_{\mathcal{T}}$, such as $\mathcal{X}_{\mathcal{P},R}$ formed from a partition, it may take some work to argue that X is an SFT, for it is possible that X has forbidden patterns in addition to the invalid horizontal and vertical pairings of prototiles.

A.2. Symbolic Representations and Markov Partitions. Here we will give precise definition to the term *Markov partition*. Suppose that (M, \mathbb{Z}^2, R) is a topological dynamical system where M is a compact topological space. Recall that a *topological partition* of M is a collection $\mathcal{P} = \{P_0, P_1, \dots, P_{n-1}\}$ of disjoint open sets such that $M = \overline{P_0} \cup \overline{P_1} \cup \dots \cup \overline{P_{n-1}}$. Let $\mathcal{A} = \{0, 1, \dots, r-1\}$. For any finite set $S \subset \mathbb{Z}^2$, let $\mathcal{A}^S = \{x: S \rightarrow \mathcal{A}\}$. A *pattern* $x \in \mathcal{A}^S$ is *allowed* for \mathcal{P}, R if

$$\bigcap_{\mathbf{k} \in S} R^{-\mathbf{k}}(P_{w_{\mathbf{k}}}) \neq \emptyset.$$

We denote the set of all allowed patterns for \mathcal{P} and R by $\mathcal{L}_{\mathcal{P},R}$. Labbé points out in [Lab21] that $\mathcal{L}_{\mathcal{P},R}$ is the language of a subshift of $\mathcal{X}_{\mathcal{P},R} \subseteq \mathcal{A}^{\mathbb{Z}^2}$ and leads to the following definition.

Definition A.1. *Let*

$$\mathcal{X}_{\mathcal{P},R} = \{x \in \mathcal{A}^{\mathbb{Z}^2} \mid \pi_S \circ \sigma^{\mathbf{n}}(x) \in \mathcal{L}_{\mathcal{P},R} \text{ for every } \mathbf{n} \in \mathbb{Z}^2 \text{ and finite subset } S \subset \mathbb{Z}^2\}.$$

*We call $\mathcal{X}_{\mathcal{P},R}$ the **symbolic dynamical system** corresponding to \mathcal{P}, R .*

For $w \in \mathcal{X}_{\mathcal{P},R} \subset \mathcal{A}^{\mathbb{Z}^2}$ and $n \geq 0$, define

$$D_n(w) = \bigcap_{\|\mathbf{k}\| \leq n} R^{-\mathbf{k}}(P_{w_{\mathbf{k}}}) \subseteq M.$$

We see that $\overline{D_n}(w)$ is compact and $\overline{D_n}(w) \supseteq \overline{D_{n+1}}(w)$ for each $n \geq 0$, and consequently, $\bigcap_{n=0}^{\infty} \overline{D_n}(w) \neq \emptyset$.

The hope is that configurations $x \in \mathcal{X}_{\mathcal{P},R}$ are generated uniquely as orbits of points in M , and the above intersection being a single point guarantees this:

Definition A.2. *A topological partition \mathcal{P} of M gives a **symbolic representation** of (M, \mathbb{Z}^2, R) if for every $w \in \mathcal{X}_{\mathcal{P},R}$, the intersection $\bigcap_{n=0}^{\infty} \overline{D_n}(w)$ consists of exactly one point $m \in M$. The configuration $w \in \mathcal{X}_{\mathcal{P},R}$ is called a **symbolic representation** of $m \in M$.*

Labbé provides the following alternative criterion for determining when a partition gives a symbolic representation.

Lemma A.3 ([Lab21]). *Let (M, \mathbb{Z}^2, R) be a minimal dynamical system and $\mathcal{P} = \{P_0, P_1, \dots, P_{r-1}\}$ be a topological partition of M . If there exists an atom P_i which is invariant only under the trivial translation in M , then \mathcal{P} gives a symbolic representation of (M, \mathbb{Z}^2, R) .*

The following definition is taken from [Lab21].

Definition A.4. *A topological partition \mathcal{P} of M is a **Markov partition** for (M, \mathbb{Z}^2, R) if*

- \mathcal{P} gives a symbolic representation of (M, \mathbb{Z}^2, R) and
- $\mathcal{X}_{\mathcal{P}, R}$ is a shift of finite type (SFT).

A.3. Conjugacy and Factor Maps. With (M, \mathbb{Z}^2, R) and \mathcal{P} encoding a space of configurations $(\mathcal{X}_{\mathcal{P}, R}, \mathbb{Z}^2, \sigma)$, it is natural to consider morphisms from (M, \mathbb{Z}^2, R) to $(\mathcal{X}_{\mathcal{P}, R}, \mathbb{Z}^2, \sigma)$ and vice versa. Let (X, G, S) and (Y, G, T) be topological dynamical systems having the same group G . A **homomorphism** of dynamical systems is a continuous map $f: X \rightarrow Y$ such that $T^g \circ f = f \circ S^g$ for all $g \in G$. If f is a homomorphism, we call f an **embedding** if it is one-to-one; we call f a **factor map** if it is onto, in which case we call Y a **factor** of X and X an **extension** of Y ; and we call f a **topological conjugacy** if it is bijective with continuous inverse, in which case we say (X, G, S) and (Y, G, T) are **topologically conjugate**.

A.4. From Symbolic Representations to Wang Shifts. Here we borrow more theory from [Lab21]. The idea that we want to make precise is that when \mathcal{P} gives a symbolic representation of (M, \mathbb{Z}^2, R) , there is a protoset \mathcal{T} such that $\mathcal{X}_{\mathcal{P}, R} \subset \Omega_{\mathcal{T}}$; if \mathcal{T} happens to be the protoset of interest (i.e., the protoset you used to generate the dot pattern which in turn you used to form \mathcal{P}), then we have necessary result that orbits of points under the action of R in M and the partition \mathcal{P} encode valid tilings.

Suppose $\mathcal{P} = \{P_a\}_{a \in \mathcal{A}}$ is a topological partition of the 2-dimensional torus \mathbf{T} , and suppose that \mathcal{P} gives a symbolic representation of $(\mathbf{T}, \mathbb{Z}^2, R)$. The **boundary** of \mathcal{P} is the set

$$\Delta = \bigcup_{a \in \mathcal{A}} \partial P_a,$$

and

$$\Delta_{\mathcal{P}, R} = \bigcup_{\mathbf{n} \in \mathbb{Z}^2} R^{\mathbf{n}}(\Delta) \subset \mathbf{T}.$$

is the set of points in \mathbf{T} whose orbits intersect Δ . It can be seen that $\mathbf{T} \setminus \Delta_{\mathcal{P}, R}$ is dense in \mathbf{T} . We will assume that Δ consists of straight line segments.

We get the following from [Lab21]:

Proposition A.5. [Lab21, Prop. 5.1] *Let \mathcal{P} give a symbolic representation of the dynamical system $(\mathbf{T}, \mathbb{Z}^2, R)$ such that R is a \mathbb{Z}^2 -rotation on \mathbf{T} . Let $f: \mathcal{X}_{\mathcal{P}, R} \rightarrow \mathbf{T}$ be defined such that $f(w)$ is the unique point in the intersection $\bigcap_{n=0}^{\infty} \overline{D}_n(w)$. The map f is a factor map from $(\mathcal{X}_{\mathcal{P}, R}, \mathbb{Z}^2, \sigma)$ to $(\mathbf{T}, \mathbb{Z}^2, R)$ such that $R^{\mathbf{k}} \circ f = f \circ \sigma^{\mathbf{k}}$ for every $\mathbf{k} \in \mathbb{Z}^2$. The map f is one-to-one on $f^{-1}(\mathbf{T} \setminus \Delta_{\mathcal{P}, R})$.*

Following Section 4 of [Lab21], for each $\mathbf{x} \in \mathbf{T} \setminus \Delta_{\mathcal{P}, R}$, we define a map $\text{CFG}_{\mathbf{x}}^{\mathcal{P}, R}: \mathbb{Z}^2 \rightarrow \mathcal{A}$ by

$$\text{CFG}_{\mathbf{x}}^{\mathcal{P}, R}(\mathbf{n}) = a \quad \text{if and only if} \quad R^{\mathbf{n}}(\mathbf{x}) \in P_a$$

(“CFG” for “configuration”). $\text{CFG}_{\mathbf{x}}^{\mathcal{P}, R}$ gives rise to a map $\text{SR}: \mathbf{T} \setminus \Delta_{\mathcal{P}, R} \rightarrow \mathcal{A}^{\mathbb{Z}^2}$ defined by

$$\text{SR}(\mathbf{x}) = \text{CFG}_{\mathbf{x}}^{\mathcal{P}, R}$$

(“SR” for “symbolic representation”). Next, we wish to extend SR to a map on all \mathbf{T} , including $\Delta_{\mathcal{P}, R}$. This is accomplished by choosing a direction \mathbf{v} that is not parallel to any of the lines comprising Δ , and then defining $\text{SR}^{\mathbf{v}}: \mathbf{T} \rightarrow \mathcal{A}^{\mathbb{Z}^2}$ by

$$\text{SR}^{\mathbf{v}}(\mathbf{x}) = \lim_{\varepsilon \rightarrow 0^+} \text{SR}(\mathbf{x} + \varepsilon \mathbf{v}).$$

The idea here is that if $R^n(\mathbf{x}) \in \Delta$, there is ambiguity as to which atom's label is assigned to \mathbf{n} by CFG; the direction \mathbf{v} settles that ambiguity by assigning to \mathbf{n} the label of the atom on the \mathbf{v} side of Δ where $R^n(\mathbf{x})$ lies.

The following lemma from [Lab21] characterizes $\mathcal{X}_{\mathcal{P},R}$ in terms of map SR.

Lemma A.6. *For each direction \mathbf{v} not parallel to a line segment in Δ , we have*

$$\overline{\text{SR}^{\mathbf{v}}(\mathbf{T})} = \overline{\text{SR}(\mathbf{T} \setminus \Delta_{\mathcal{P},R})} = \mathcal{X}_{\mathcal{P},R}$$

where the overline indicates topological closure in the compact product topology on $\mathcal{A}^{\mathbb{Z}^2}$.

We summarize further pertinent results from [Lab21] here:

- (1) $\text{SR}^{\mathbf{v}} : \mathbf{T} \rightarrow \mathcal{X}_{\mathcal{P},R}$ is 1-1, and so
- (2) the inverse map can be extended to the factor map $f : \mathcal{X}_{\mathcal{P},R} \rightarrow \mathbf{T}$ such that for each configuration $\omega \in \mathcal{X}_{\mathcal{P},R}$, $f(\omega) = \bigcap_{n=0}^{\infty} \overline{D_n \omega}$ (so f is as defined in Proposition A.5).
- (3) f is 1-1 on $f^{-1}(\mathbf{T} \setminus \Delta_{\mathcal{P},R})$.
- (4) The factor map commutes the shift actions R on \mathbf{T} and σ on $\mathcal{X}_{\mathcal{P},R}$; that is, $R^n f = f \sigma^n$.

Using the factor map f and these properties of f , Labbé proved the following important fact [Lab21]:

Lemma A.7. *Suppose \mathcal{P} gives a symbolic representation of $(\mathbf{T}, \mathbb{Z}^2, R)$. Then*

- (1) *if $(\mathbf{T}, \mathbb{Z}^2, R)$ is minimal, then $(\mathcal{X}_{\mathcal{P},R}, \mathbb{Z}^2, \sigma)$ is minimal, and*
- (2) *if R is a free \mathbb{Z}^2 -action on \mathbf{T} , then $\mathcal{X}_{\mathcal{P},R}$ is aperiodic.*

The last results we quote from [Lab21] pertain to understanding how a topological partition \mathcal{P} gives rise to Wang tile protoset \mathcal{T} such that $\mathcal{X}_{\mathcal{P},R} \subset \Omega_{\mathcal{T}}$. To that end, suppose that $(\mathbf{T}, \mathbb{Z}^2, R)$ is a dynamical system, let $\mathcal{P}_r = \{P_i\}_{i \in I}$ (the *right side partition*) and $\mathcal{P}_b = \{P_j\}_{j \in J}$ (the *bottom side partition*) be two finite topological partitions of \mathbf{T} , and then let $\mathcal{P}_l = \{R^{(1,0)}(P_a) : P_a \in \mathcal{P}_r\}$ (the *left side partition*) and $\mathcal{P}_t = \{R^{(0,1)}(P_a) : P_a \in \mathcal{P}_l\}$ (the *top side partition*); the labels of the atoms of \mathcal{P}_l and \mathcal{P}_r (i.e. the set I) are the colors of the right and left sides of tiles in a soon-to-be-defined Wang tile protoset, and the labels of the atoms of \mathcal{P}_b and \mathcal{P}_t (i.e. the set J) are the colors of the top and bottom sides in that same Wang tile protoset. For each $(i, j, k, \ell) \in I \times J \times I \times J$, let

$$P_{(i,j,k,\ell)} = P_i \cap P_j \cap P_k \cap P_\ell.$$

Next, define

$$\mathcal{T} = \{\tau \in I \times J \times I \times J : P_\tau \neq \emptyset\}.$$

We interpret each $\tau \in \mathcal{T}$ as a Wang tile as described in Section 2.1. \mathcal{T} is naturally associated with the *tile partition* $\mathcal{P} = \{P_\tau : \tau \in \mathcal{T}\}$ which is the refinement of $\mathcal{P}_l, \mathcal{P}_r, \mathcal{P}_b$ and \mathcal{P}_t , and each point $\mathbf{x} \in \mathbf{T} \setminus \Delta$ corresponds to a unique tile in \mathcal{T} . With \mathcal{P} defined as a partition of the torus \mathcal{T} in this way, we find the following lemmas in [Lab21].

Lemma A.8. *With \mathcal{P} defined as above as a refinement of $\mathcal{P}_l, \mathcal{P}_r, \mathcal{P}_b$, and \mathcal{P}_t , we have $\mathcal{X}_{\mathcal{P},R} \subseteq \Omega_{\mathcal{T}}$.*

Lemma A.9. *For every direction \mathbf{v} not parallel to a line segment in Δ , $\text{SR}^{\mathbf{v}} : \mathbf{T} \rightarrow \Omega_{\mathcal{T}}$ is a one-to-one map.*

B. APPLICATION OF LABBÉ'S THEORY TO EXPERIMENTALLY DETERMINED PARTITIONS

In this section, we apply the theory as outlined in A to the partition \mathcal{P}_{16} corresponding to the Ammann A2-derived Wang protoset \mathcal{T}_{16} . Let us begin by pointing out that it is easily checked that the partition \mathcal{P}_{16} is the refinement of the partitions $\mathcal{P}_{16,t}, \mathcal{P}_{16,\ell}, \mathcal{P}_{16,b}$, and $\mathcal{P}_{16,r}$, as depicted in Figure 28, and so by Lemma A.8, we know that $\mathcal{X}_{\mathcal{P}_{16},R_{16}} \subseteq \Omega_{16}$.

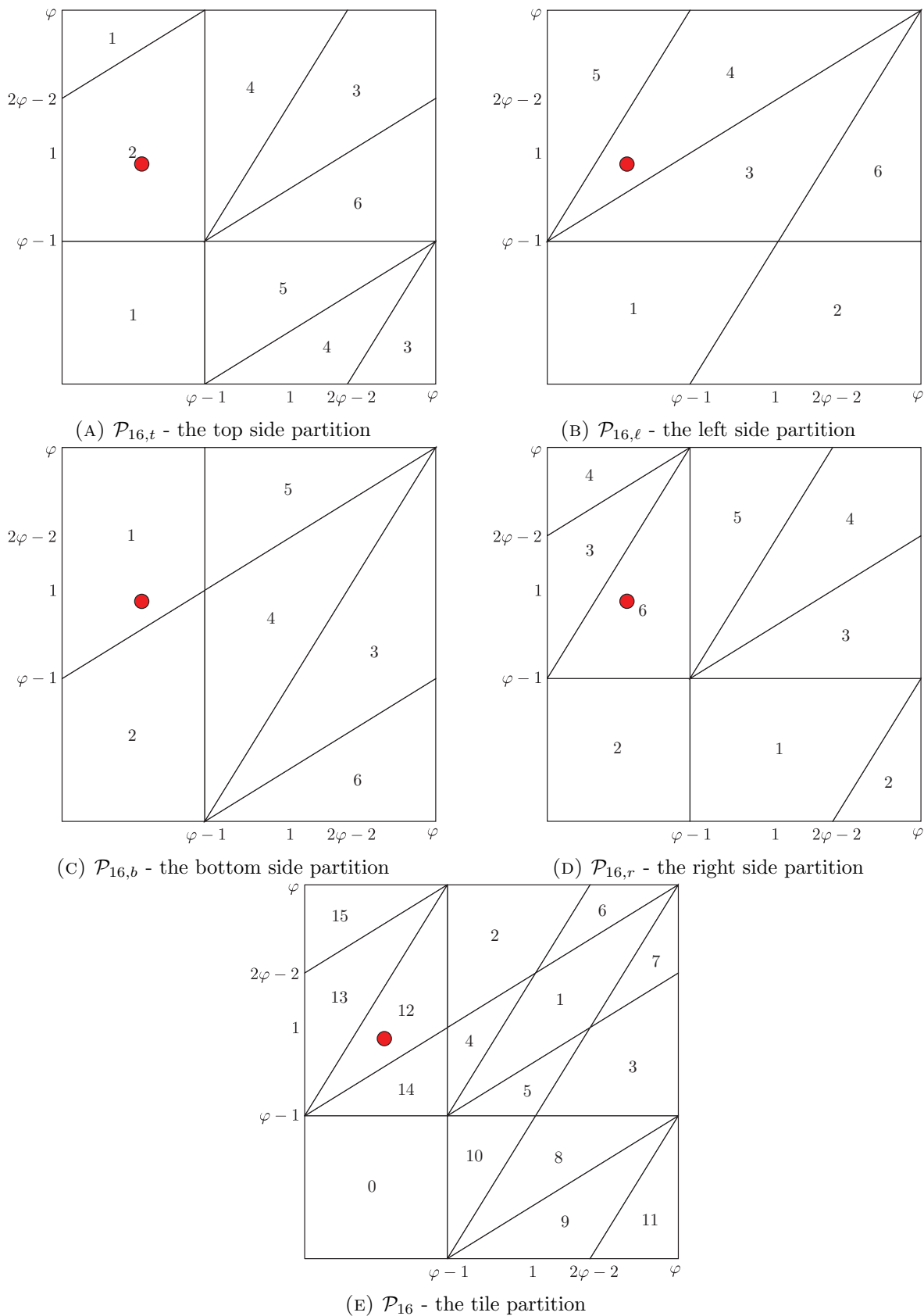


FIGURE 28. Refining the side partitions to obtain the tile partition \mathcal{P} . The red dot corresponds to the tile $(r, t, l, b) = (6, 2, 4, 1)$, which is tile 12 from Figure 11, so the corresponding region in \mathcal{P}_{16} which is the intersection of the regions containing the red dot, is labeled 12.

Next, we want to demonstrate that \mathcal{P} gives a symbolic representation of $(\mathbf{T}_{16}, \mathbb{Z}^2, \mathbb{R}_{16})$, but we will first establish a few supporting results.

Lemma B.1. *Let $\mathbf{v} = (v_x, v_y) \in \mathbf{T}_{16} = [0, \varphi] \times [0, \varphi]$ and let $x_0, x_1 \in [0, \varphi]$ with $x_0 < x_1$. Then, there exists some $\mathbf{v}' = (v'_x, v'_y) \in \mathcal{O}_{R_{16}}(\mathbf{v})$ with $x_0 < v'_x < x_1$.*

Proof. Consider the set $\{R_{16}^{(n,0)}(\mathbf{v}) : n \in \mathbb{Z}\} = \{(v_x + n \pmod{\varphi}, v_y) : n \in \mathbb{Z}\} \subset \mathcal{O}_{R_{16}}(\mathbf{v})$, which we see is an irrational rotation of the point \mathbf{v} horizontally around \mathbf{T}_{16} . Consequently, $\{R_{16}^{(0,n)}(\mathbf{v}) : n \in \mathbb{Z}\}$ is dense on the horizontal line through \mathbf{v} , and it follows that there exists some $\mathbf{v}' = (v'_x, v'_y) \in \mathcal{O}_{R_{16}}(\mathbf{v})$ with $x_0 < v'_x < x_1$. \square

In an analogous way, we can prove the following Lemma:

Lemma B.2. *Let $\mathbf{v} = (v_x, v_y) \in \mathbf{T}_{16}$ and let $y_0, y_1 \in [0, \varphi]$ with $y_0 < y_1$. Then there exists some $\mathbf{v}' = (v_x, v'_y) \in \mathcal{O}_{R_{16}}(\mathbf{v})$ with $y_0 < v'_y < y_1$.*

Lemmas B.1 and B.2 show that the orbit of any point in \mathbf{T}_{16} has a non-empty intersection with any horizontal or vertical strip on the torus, which allows us to prove the following theorem.

Proposition B.3. *$(\mathbf{T}_{16}, \mathbb{Z}^2, R_{16})$ is minimal.*

Proof. We show that for arbitrary $\mathbf{p} = (p_x, p_y) \in \mathbf{T}_{16}$, $\mathcal{O}_{R_{16}}(\mathbf{p})$ is dense in \mathbf{T}_{16} . Let $\mathbf{a} \in \mathbf{T}_{16}$ and let U be an open square of side length 2ε centered at $\mathbf{a} = (a_x, a_y)$ in \mathbf{T} , and without loss of generality, choose ε sufficiently small so that $0 < a_x - \varepsilon < a_x + \varepsilon < \varphi$ and $0 < a_y - \varepsilon < a_y + \varepsilon < \varphi$. By Lemma B.2, there exists $n \in \mathbb{Z}$ such that $\mathbf{p}' = (p_x, p'_y) = R^{(0,n)}(\mathbf{p})$ lies in the horizontal strip bounded by lines $y = a_y - \varepsilon$ and $y = a_y + \varepsilon$. Next, by Lemma B.1, there exists some $m \in \mathbb{Z}$ such that $\mathbf{p}'' = R^{(m,n)}(\mathbf{p}') = (p'_x, p'_y)$ with $a_x - \varepsilon < p'_x < a_x + \varepsilon$, and so we see that $\mathbf{p}'' \in U$, and so $\mathcal{O}_R(\mathbf{p}) \cap U \neq \emptyset$. \square

To prove that \mathcal{P} gives a symbolic representation of $(\mathbf{T}, \mathbb{Z}^2, R)$, We apply Lemma A.3, showing that some atom of \mathcal{P} is invariant only under the trivial translation.

Proposition B.4. *\mathcal{P}_{16} gives a symbolic representation of $(\mathbf{T}_{16}, \mathbb{Z}^2, R_{16})$.*

Proof. Consider $P_0 \in \mathcal{P}_{16}$ from Figure 14. We show that P_0 is invariant only under the trivial translation under R_{16} . If $R_{16}^{\mathbf{n}}(P_0) = P_0$ for some $\mathbf{n} = (n_1, n_2) \in \mathbb{Z}^2$, then by continuity $R^{\mathbf{n}}$ must fix $(0, 0) \in \mathbf{T}_{16}$, from which we obtain $n_1 \pmod{\varphi} = 0$ and $n_2 \pmod{\varphi} = 0$. Due to the irrationality of φ , we conclude that $n_1 = n_2 = 0$, so $R^{\mathbf{n}}$ is the trivial translation. \square

Having established that \mathcal{P}_{16} gives a symbolic representation of $(\mathbf{T}_{16}, \mathbb{Z}^2, R_{16})$, we then apply Lemma A.7 to conclude that $(\mathcal{X}_{\mathcal{P}_{16}, R_{16}}, \mathbb{Z}^2, \sigma)$ is minimal and $\mathcal{X}_{\mathcal{P}_{16}, R_{16}}$ is an aperiodic subshift of Ω_{16} . Moreover, we point out that it was recently proven by Labbé [Lab24][Lemma 11.7] that Ω_{16} is minimal. It follows that $\mathcal{X}_{\mathcal{P}_{16}, R_{16}} = \Omega_{16}$, and so $\mathcal{X}_{\mathcal{P}_{16}, R_{16}}$ is an SFT, proving the following.

Theorem B.5. *\mathcal{P}_{16} is a Markov partition for $(\mathbf{T}_{16}, \mathbb{Z}^2, \mathbb{R}_{16})$, $\mathcal{X}_{\mathcal{P}_{16}, R_{16}}$ is aperiodic, and $\mathcal{X}_{\mathcal{P}_{16}, R_{16}} = \Omega_{16}$.*

REFERENCES

- [Wan61] Hao Wang. “Proving Theorems by Pattern Recognition — II”. In: *Bell System Technical Journal* 40.1 (1961), pp. 1–41. DOI: <https://doi.org/10.1002/j.1538-7305.1961.tb03975.x>. eprint: <https://onlinelibrary.wiley.com/doi/pdf/10.1002/j.1538-7305.1961.tb03975.x>. URL: <https://onlinelibrary.wiley.com/doi/abs/10.1002/j.1538-7305.1961.tb03975.x>.
- [Ber65] Robert Berger. *THE UNDECIDABILITY OF THE DOMINO PROBLEM*. Thesis (Ph.D.)—Harvard University. ProQuest LLC, Ann Arbor, MI, 1965, (no paging). URL: http://gateway.proquest.com/openurl?url_ver=Z39.88-2004&rft_val_fmt=info:ofi/fmt:kev:mtx:dissertation&res_dat=xri:pqdiss&rft_dat=xri:pqdiss:0248356.

- [Ber66] Robert Berger. “The undecidability of the domino problem”. In: *Mem. Amer. Math. Soc.* 66 (1966), p. 72. ISSN: 0065-9266.
- [GS87] Branko Grünbaum and G. C. Shephard. *Tilings and Patterns*. New York: W. H. Freeman and Company, 1987.
- [Gar97] Martin Gardner. *Penrose tiles to trapdoor ciphers*. MAA Spectrum. . . and the return of Dr. Matrix, Revised reprint of the 1989 original. Mathematical Association of America, Washington, DC, 1997, pp. x+319. ISBN: 0-88385-521-6.
- [Jan21] Hyeun Jang. “Directional Expansiveness”. PhD thesis. Washington D.C., 2021.
- [JR21] Emmanuel Jeandel and Michaël Rao. “An aperiodic set of 11 Wang tiles”. In: *Advances in Combinatorics* (Jan. 2021). ISSN: 2517-5599. DOI: 10.19086/aic.18614. URL: <http://dx.doi.org/10.19086/aic.18614>.
- [Lab21] Sébastien Labbé. “Markov partitions for toral \mathbb{Z}^2 -rotations featuring Jeandel–Rao Wang shift and model sets”. In: *Annales Henri Lebesgue* 4 (Jan. 2021), pp. 283–324. DOI: 10.5802/ahl.73. URL: <https://doi.org/10.5802/ahl.73>.
- [LMM22] Sébastien Labbé, Casey Mann, and Jennifer McLoud-Mann. *Nonexpansive directions in the Jeandel-Rao Wang shift*. 2022. DOI: 10.48550/ARXIV.2206.02414. URL: <https://arxiv.org/abs/2206.02414>.
- [Lab23] Sébastien Labbé. *slabbe Package for SageMath*. Version 0.7.6. 2023. URL: <https://pypi.org/project/slabbe/>.
- [Smi+23a] David Smith et al. *A chiral aperiodic monotile*. 2023. arXiv: 2305.17743 [math.CO].
- [Smi+23b] David Smith et al. *An aperiodic monotile*. 2023. arXiv: 2303.10798 [math.CO].
- [Lab24] Sébastien Labbé. *Metallic mean Wang tiles I: self-similarity, aperiodicity and minimality*. 2024. arXiv: 2312.03652 [math.DS].

(H. Hults) UNIVERSITY OF WASHINGTON BOTHELL, 18115 CAMPUS WAY NE, BOTHELL, WA 98011-8246
Email address: hkhults@uw.edu

(H. Jitsukawa) TUFTS UNIVERSITY, 419 BOSTON AVE, MEDFORD, MA 02155
Email address: hikaru.jitsukawa@tufts.edu

(C. Mann) UNIVERSITY OF WASHINGTON BOTHELL, 18115 CAMPUS WAY NE, BOTHELL, WA 98011-8246
Email address: cemann@uw.edu

(J. Zhang) GEORGIA INSTITUTE OF TECHNOLOGY, NORTH AVE NW, ATLANTA, GA 30332 -
Email address: jzhang3264@gatech.edu